

**Diffusion Behaviour of Nuclides Considering Pathways
in Fractured Crystalline Rocks**

August 1997

Tokai Works

Power Reactor and Nuclear Fuel Development Corporation

複製又はこの資料の入手については、下記にお問い合わせ下さい。

〒319-11 茨城県那珂郡東海村大字村松 4 - 33

動力炉・核燃料開発事業団 東海事業所

技術開発推進部・技術管理室

Inquiries about copyright and reproduction should be addressed to :
Technology Management Section Tokai Works Power Reactor and
Nuclear Fuel Development Corporation Tokai 4 - 33, Muramatsu,
Tokai - mura, Naka - gun, Ibaraki - ken 319 - 11, Japan

動力炉・核燃料開発事業団 (Power Reactor and Nuclear Fuel Development
Corporation) 1997

物質移行経路を考慮した割れ目を含む結晶質岩中の 核種の拡散挙動

佐藤治夫*, 澁谷朝紀*, 舘幸男*,
太田久二雄**, 天野健治***, 油井三和*

要 旨

高レベル放射性廃棄物地層処分の性能評価研究において、核種の移行遅延特性を定量的に調べモデル化することは重要な課題の1つとして挙げられている。筆者らは、結晶質岩中における核種の遅延の程度を定量化するため、割れ目から岩石マトリックス方向への核種の拡散、岩石への核種の収着および間隙特性の変化について調べている。本研究では、釜石原位置試験場の花崗閃緑岩割れ目周辺に見られる割れ目充填鉱物部および変質部の内、地下水が接触している割れ目を対象に核種の移行遅延特性を調べた。イオン電荷をパラメーターにNa, Cs, HTO, Cl, Seについて22~25℃の範囲で見掛けの拡散係数および実効拡散係数を取得した。透過拡散法により、割れ目充填鉱物部、変質部、花崗閃緑岩に対して取得すると共に、Cs, Sr, Se, ^{238}U および ^{239}Pu のバッチ法による収着実験を同岩石について行い、分配係数を取得した。酸化還元条件に鋭敏な元素の内、Seについてのみ N_2 雰囲気グローブボックス ($\text{O}_2 < 1\text{ppm}$) 内で行い、他の元素は大気雰囲気で行った。岩石試料と同じ場所から採取した地下水 (pH8.7~9.5) を実験では用いた。岩石試料の間隙率および密度を水中飽和法および水銀圧入法により、また、細孔径分布や比表面積を水銀圧入法により測定した。間隙率は、割れ目充填鉱物部 (5.6%) > 変質部 (3.2%) > 花崗閃緑岩 (2.3%) の順で小さくなり、割れ目からマトリックス方向に対して小さくなるのが分かった。花崗閃緑岩および変質部の細孔径分布は10nm~0.2mmの範囲にわたっており、割れ目充填鉱物部は50nm~0.2mmの範囲であった。しかしながら、割れ目充填鉱物部における多くの細孔径は100nmと0.2mm付近で見られた。全てのイオン (Na^+ , Cs^+ , HTO, Cl^- , SeO_3^{2-}) の実効拡散係数は間隙率に依存し、割れ目充填鉱物部 > 変質部 > 花崗閃緑岩の順に小さくなった。細孔径分布の測定結果から間隙径がイオン径に比べて大きく、岩石表面とイオンとの静電的相互作用の効果はそれほど大きくないものと考えられることから、岩石マトリックス中のイオンの実効拡散係数を間隙率や屈曲度などの間隙構造因子および自由水中のイオンの拡散係数を用いて予測した。その結果、予測値は実測値とほぼ一致し、形状因子に基づいたモデルの適用性が確認された。また、岩石に対するCsおよびSrの分配係数は、割れ目充填鉱物部 > 花崗閃緑岩 \cong 変質部の順となり、Seは全ての岩石に対してほとんど収着しない結果となった。Uの分配係数には液固比依存性が見られ、液固比100ml·g⁻¹ではほとんど収着しない結果となったのに対し、液固比1000ml·g⁻¹では有意な分配係数が認められており、その値は、割れ目充填鉱物部 > 変質部 > 花崗閃緑岩の順となった。一方、Puの分配係数はUとは逆の傾向となった。

* 東海事業所 環境技術開発部 地層処分開発室
** 東濃地科学センター 地質環境研究室
*** 釜石事務所

CONTENTS

ABSTRACT	1
1. INTRODUCTION	3
2. EXPERIMENTALS	5
2.1 Location of the Kamaishi In Situ Test Site	5
2.2 Items carried out in this study	5
2.3 Diffusion experiments	7
2.3.1 Experiments for Na, Cs and Cl	10
2.3.2 Experiments for Se	11
2.3.3 Experiments for HTO	11
2.4 Batch sorption experiments	12
2.4.1 Sorption experiments for Cs, Sr and ²³⁸ U	14
2.4.2 Sorption experiments for Se	15
2.4.3 Sorption experiments for ²³⁹ Pu	15
2.5 CEC measurements	15
2.6 Measurements of porosity and pore-size distribution in rock matrixes ---	16
2.6.1 Water saturation method	17
2.6.2 Mercury porosimetry	17
3. RESULTS	19
3.1 Diffusion coefficients	19
3.2 Distribution coefficients	25
3.3 CEC values of the rock specimens	26
3.4 Porosity and pore-size distribution in rock	28
4. DISCUSSION	32
4.1 Relation between diffusion coefficients and porosities	32
4.2 Relation between K _d and CEC values	42
4.3 Consideration of a simplified model for D _e	43

5. CONCLUSION	45
6. ACKNOWLEDGEMENT	46
7. REFERENCES	47

FIGURES

Figure 1 Illustration of fracture type identified in Kurihashi granodiorite --	4
Figure 2 Geological map around the Kamaishi In Situ Test Site	6
Figure 3 Schematic view of a diffusion cell	8
Figure 4 Changes in concentration of Cs in the measurement cell as a function of time for fracture fillings, altered and intact granodiorite	21
Figure 5 Correlation between porosity and rock sample	30
Figure 6 Examples of measurement in pore-size distribution by mercury porosimetry for each rock	31
Figure 7 Effective diffusion coefficients as a function of porosity	34
Figure 8 Apparent diffusion coefficients as a function of porosity	35
Figure 9 Geometric factor as a function of porosity	38
Figure 10 Formation factors of the rocks as a function of porosity	39
Figure 11 Comparison between De values predicted by the model and measured De values	44

TABLES

Table 1 Experimental conditions in the diffusion experiments	9
Table 2 Chemical compositions of the in situ groundwater	9
Table 3 Experimental conditions for sorption experiments	13

Table 4	Average apparent and effective diffusion coefficients estimated for each ion -----	24
Table 5	Experimental results for sorption -----	25
Table 6	The CEC and leaching ions -----	27
Table 7	Porosities, dry densities and specific surface area of pores for each rock -----	29
Table 8	Comparison between distribution coefficients obtained from both diffusion and batch sorption experiments -----	41

APPENDIX

Appendix 1	Summary of parameters -----	50
Appendix 2	CEC and leaching ions -----	52
Appendix 3	Relation between CEC values and rock facies -----	53
Appendix 4	Sorption parameters -----	54
Appendix 5	Pore parameters -----	57

Diffusion Behaviour of Nuclides Considering Pathways in Fractured Crystalline Rocks

Haruo Sato*, Tomoki Shibutani*, Yukio Tachi*, Kunio Ota**,
Kenji Amano***, Mikazu Yui*

ABSTRACT

Retardation of key nuclides is one of the most important mechanisms to be examined specifically and modelled for the performance assessment of geological disposal of radioactive waste. We have been studying diffusion of nuclides into the pore spaces of the rock matrix, sorption of nuclides on the rock pore surfaces and pore properties to quantify the degree of nuclide retardation in fractured crystalline rock. The work has concentrated on predominant water conducting fracture system in the host granodiorite in the Kamaishi In Situ Test Site, which consists of fracture fillings and altered granodiorite. Through-diffusion experiments to obtain effective and apparent diffusion coefficients (D_a and D_e , respectively) for Na, Cs, HTO, Cl and Se as a function of ionic charge at 22 ~ 25°C and batch sorption experiments for Cs, Sr, Se, ^{238}U and ^{239}Pu were conducted on fracture fillings, altered and intact granodiorite. The experiments only for Se, a redox sensitive element, were done in an N_2 -atmospheric glove box ($\text{O}_2 < 1\text{ppm}$) to keep the chemical species. In situ groundwater (pH8.7 ~ 9.5) sampled from the same place as rock samples was used for the experiments. Porosity and density of each rock sample were determined by both water saturation method and mercury porosimetry, and pore-size distribution and specific surface area of pores were measured by mercury porosimetry. The porosity is in the order; fracture fillings (5.6%) > altered rock (3.2%) > intact rock (2.3%). The pore-size distribution of the intact and altered granodiorite is ranging from 10nm to 0.2mm, and the fracture fillings have that of 50nm to 0.2mm, but a lot of pores were found around 100nm and 0.2mm in the fracture fillings. The effective diffusion coefficients for all species (Na^+ , Cs^+ , HTO, Cl^- , SeO_3^{2-}) are in the order of fracture fillings > altered rock > intact rock in proportion to these porosities. Effective diffusion coefficients of these species in the rock matrix were predicted by ionic diffusion coefficients in free water and the pore structural factors such as porosity and tortuosity, and compared with the measured values because the pore sizes

* Geological Isolation Technology Section, Waste Technology Development Division, Tokai Works, 4-33 Muramatsu, Tokai-mura, Ibaraki-ken 319-11, Japan

** Geological Environment Research Section, Tono Geoscience Center, 959-31, Jorinji,, Toki-shi, Gifu-ken 509-51, Japan

*** Kamaishi Site Office, 1-80 Kasshi, Kamaishi, Iwate 026, Japan

are much larger than ionic sizes from the measurements of pore-size distributions and the effect of electrostatic interaction of species with the rock pore surface is considered to be insignificant. Consequently, the predicted values were relatively consistent with the measured ones, and the availability of simplified model based on formation factor was confirmed. The distribution coefficients of Cs and Sr on the rock matrix are in the order; fracture fillings > intact granodiorite \geq altered granodiorite, and Se hardly sorbed on all rock samples. A liquid / solid ratio dependence was found in U sorption, and U hardly sorbed for a liquid / solid ratio of 100 ml·g⁻¹, but significant sorptions were recognized for a liquid / solid ratio of 1000 ml·g⁻¹. The distribution coefficients are in the order; fracture fillings > altered granodiorite > intact granodiorite. The sorption property of Pu showed the reverse order compared with that in U.

1. INTRODUCTION

In the performance assessment of geological disposal system of high-level radioactive waste in Japan, retardation behaviour of key nuclides in rock matrix is one of the important mechanisms, and the data acquisition and modelling, focused on effective and apparent diffusion coefficients (D_e and D_a , respectively) of nuclides in the rock matrix have been developed. In fractured crystalline rocks, nuclide migration takes place along the connected pores into the rock matrix from the fracture surface by diffusion and other mechanisms. Diffusion into the rock matrix is generally considered as one of the retardation processes of nuclide migration. As an example of this study, we have been studying experimentally the properties of nuclide migration into the rock matrix from the fracture surface of granodiorite which is one of the representative crystalline rocks at the Kamaishi In Situ Test Site.

Rocks are often classified as fractured or porous media from the viewpoint of the transport and modelling of radionuclides [PNC, 1993]. Fractured media are found in crystalline rocks such as granite and consolidated rocks, and the fractures are considered to be the principal pathways for nuclide migration. Porous media are able to be described by assuming that a continuously and homogeneously distributed pore space exists in sedimentary rocks such as sandstone, mudstone, tuff, etc. in which there are no fractures.

In previous study, fracture mapping for a total of 400 fractures was carried out to develop a conceptual flow-path model in the Kurihashi granodiorite at the Kamaishi In Situ Test Site, and it is already known that fractures at the Kamaishi In Situ Test Site can be classified into three types; type A with a zone of fracture fillings, type B with a zone of fracture fillings and an altered zone, type C consisting of several fractures with a zone of fracture fillings and an altered zone [Osawa et al., 1995]. **Figure 1** shows the illustration of fracture type identified in Kurihashi granodiorite [Osawa et al., 1995]. Among the fracture types, type B was predominant in the studied area with more than 60% of fractures observed in the fracture mapping [Osawa et al., 1995]. Osawa et al. [Osawa et al., 1995] have also measured distribution coefficients of U(VI) on the rock matrix under aerobic ambient conditions by batch sorption method and porosities of the intact rock matrix by a water saturation method.

However, they are insufficient to understand and model nuclide migration into the rock matrix from the fracture.

In this study, experimental studies on diffusion of ions into the pore spaces of the rock matrix, sorption of ions on the rock pore surfaces and pore properties were carried out, concentrated on the fracture type B which is a typical single fracture. This paper mainly reports the results studied experimentally on diffusion behaviour for Cs, Na, HTO, Cl and Se as a function of ionic charge and pore properties to quantify the degree of nuclide retardation in fractured crystalline rock at the Kamaishi In Situ Test Site.

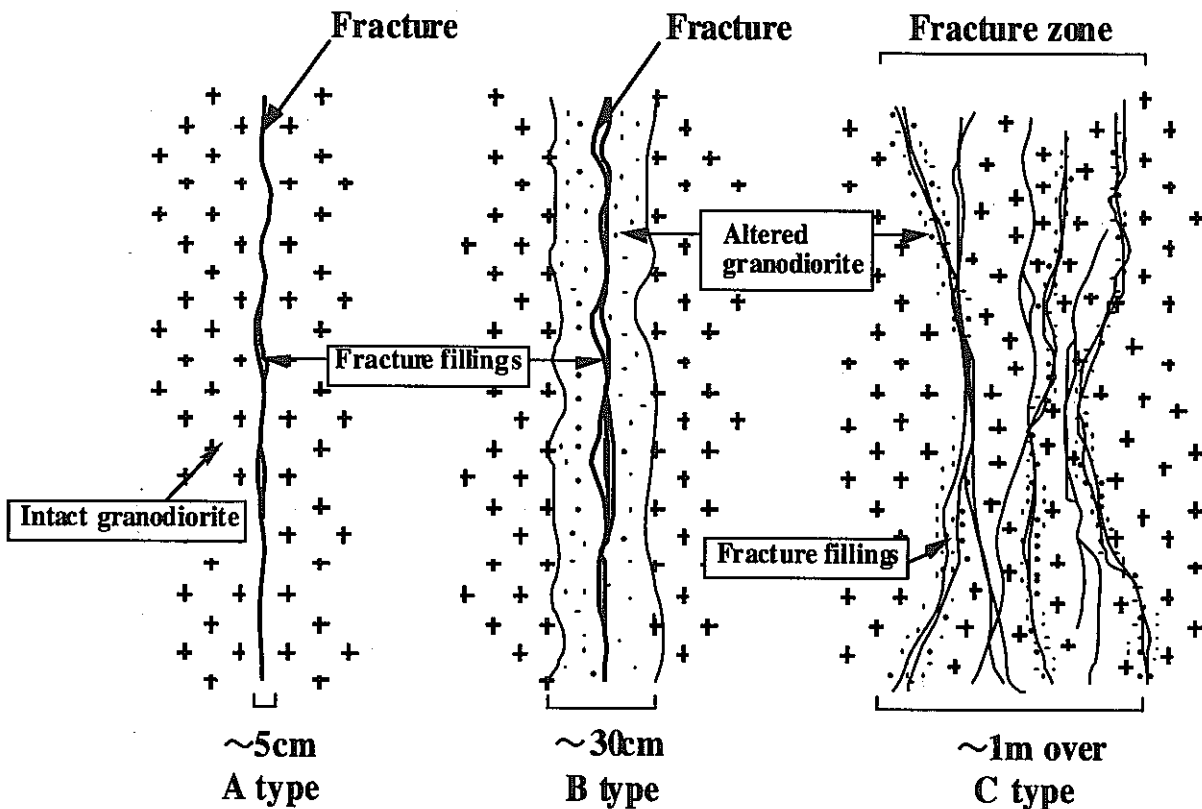


Figure 1 Illustration of fracture type identified in Kurihashi granodiorite

Fracture types A, B and C occupy about 35, 64 and 1%, respectively from fracture mapping for a total of 400 fractures in the studied area [Osawa et al., 1995].

2. EXPERIMENTALS

2.1 Location of the Kamaishi In Situ Test Site

Figure 2 shows geological map around the Kamaishi In Situ Test Site. The Kamaishi In Situ Test Site, about 20 km west of Kamaishi city downtown, is located approximately 600 km north of Tokyo and coastal area facing the Pacific Ocean. The geology of the studied area consists of Paleozoic sedimentary rock, Cretaceous sedimentary rock, the Ganidake granodiorite and the Kurihashi granodiorite [Oasawa et al., 1995]. This study was mainly carried out using both rock samples and in situ groundwater sampled from No.99 fracture which is constantly conducting with groundwater (typical fracture type B) in the drift 250m above sea level (about 700m deep from the ground surface) in the Kurihashi granodiorite. Only in the measurements of CEC, rock samples from No.148 fracture (fracture type C) were also used.

2.2 Items carried out in this study

The items conducted in this study are shown below:

- diffusion experiments for Na, Cs, HTO, Cl and Se through intact rock samples by through-diffusion method,
- batch sorption experiments for Cs, Sr, Se, ^{238}U and ^{239}Pu on crushed rock samples
- CEC measurements for rock samples
- measurements of porosity and pore-size distribution in intact rock samples by water saturation method and mercury porosimetry
- consideration of a simplified model for effective diffusion coefficients based on formation factors of the rocks and ionic diffusion coefficients in free water

In diffusion experiments, Na and Cs were used as a representative of monovalent cation, and HTO, Cl and Se were used as representatives of neutral species, monovalent and divalent anion, respectively.

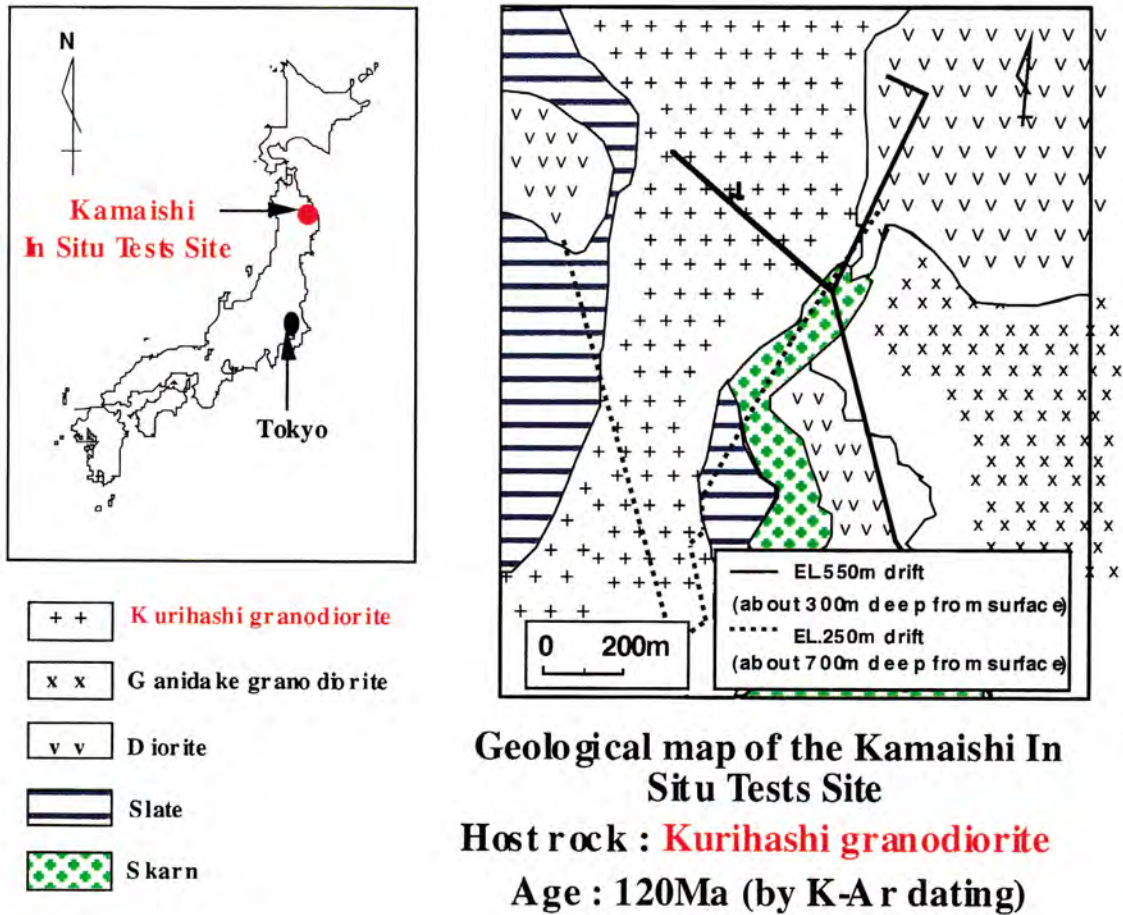


Figure 2 Geological map around the Kamaishi In Situ Test Site

The geological map shows the cross-section at 550m level.

2.3 Diffusion experiments

Through-diffusion experiments [Kita et al., 1989; Kumada et al., 1990; Park et al., 1991; Sato et al., 1992a, 1992b; Sato and Shibutani, 1994] were carried out to obtain effective and apparent diffusion coefficients (D_e and D_a , respectively) for Na, Cs, HTO, Cl and Se through three rock matrixes; fracture fillings, altered and intact granodiorite, composing fracture type B. The major mineral composition of fracture fillings is calcite and stilbite, and those of altered and intact granodiorite are quartz and plagioclase. In altered granodiorite, the rate of chlorite constituent is a little higher than that in intact granodiorite. Biotite is contained in intact granodiorite instead. The detailed mineral composition of each rock matrix is shown in the literature of Osawa et al. [Osawa et al., 1995]. **Table 1** shows the experimental conditions in the diffusion experiments. The experiments for Na, Cs and Cl were conducted at 25 °C under ambient aerobic conditions, and those for HTO were done at 23°C under the same conditions. Those for Se, a redox sensitive element, were carried out in an N₂-atmospheric glove box ($O_2 < 1\text{ppm}$) to become the valence of Se trivalent state. In situ groundwater sampled from No.99 fracture, at which place rock samples were sampled, was used as the porewater in the experiments (initial pH about 9.3, Eh vs. SHE 110mV). **Table 2** shows the chemical composition of the groundwater. The pH of the groundwater was monitored during the experiments. An acrylic diffusion cell was used for the experiments. **Figure 3** shows a schematic view of the diffusion cell. The diffusion cell is composed of two cells, a tracer and a measurement cell. A rock sample with the size of 30mm in diameter and 5mm in thickness was placed between the cells. Before the experiments, the samples were saturated with the groundwater under low pressure conditions (about 30 torr) for about a month.

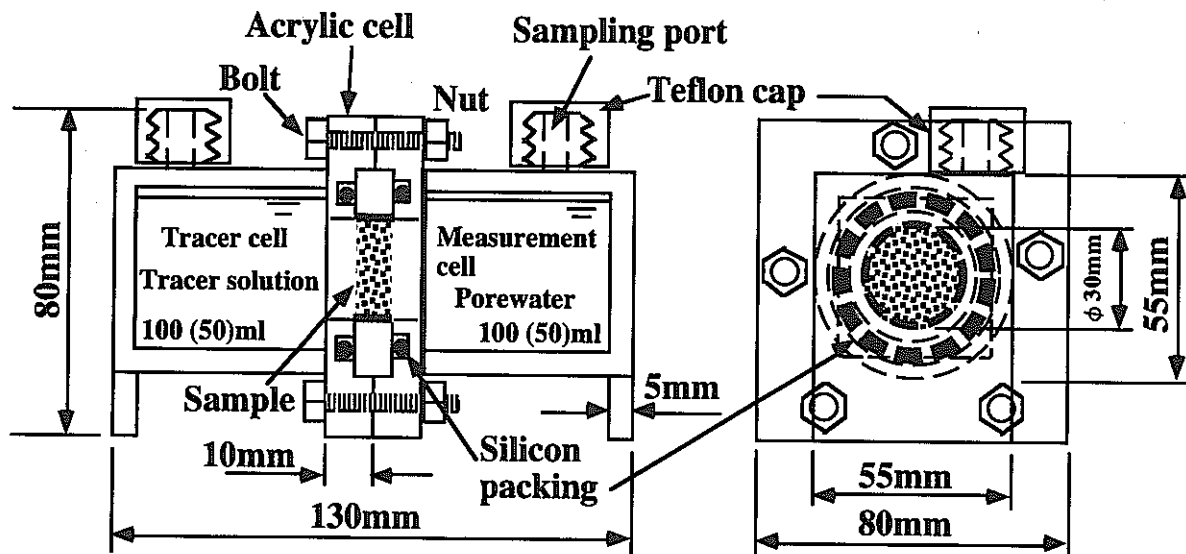


Figure 3 Schematic view of a diffusion cell

A rock sample with the size of 30 mm in diameter and 5 mm in thickness is placed between the tracer and measurement cell.

Table 1 Experimental conditions in the diffusion experiments

Rock	intact granodiorite, altered granodiorite, fracture fillings				
Tracer	Cs	Na	Cl	HTO	Se
Concentration	0.01M (1330ppm)	0.05M (1150ppm)	0.06M (2127ppm)	6000Bq/ml	6.0x10 ⁻⁴ M (50ppm)
Atmosphere	← aerobic conditions →			N ₂ -atmosphere (O ₂ < 1ppm)	
Temperature	25°C (thermobath)		23°C (room)	22°C (glove box)	
Porewater	← in situ groundwater →				
Experimental period	← 30 days →		23 days	36 days	
Producibility	← 3 →				

Table 2 Chemical compositions of the in situ groundwater

Element(ion)	Na	K	Ca	Si	F ⁻	Cl ⁻	SO ₄ ²⁻	CO ₃ ²⁻	HCO ₃ ⁻
Concentration (ppm)	9.60	0.20	5.62	5.73	0.07	1.98	9.08	3.2	22.3

2.3.1 Experiments for Na, Cs and Cl

A diffusion cell which is composed of a tracer and a measurement cell with a volume of 100ml was used in the diffusion experiments. After diffusion cell was washed with a neutral detergent, and a disc-shaped rock specimen was set between both cells. A 100ml of groundwater was then injected into both cells to saturate the rock sample. The saturation was continued for a month under low pressure conditions (about 30 torr). A tracer solution was prepared by dissolving a mixture of an NaCl and a CsCl powder in the groundwater so as to obtain certain concentration as shown in **Table 1** for each element. After saturation of the rock, the groundwater in the tracer cell was exchanged with the tracer solution prepared, and then the experiment was started. Samples, 10ml, were periodically taken from the measurement cell, and an identical volume of groundwater was added to the measurement cell to keep the solution volume constantly. Samples, 0.1ml, were also extracted from the tracer cell to check the concentration of tracer in this cell and diluted 100 times with distilled water. The pH of the solutions in the measurement and tracer cell was measured at every sampling. The diffusion cells were placed in a thermobath kept at 25°C except for sampling and pH measurements. The samples were analysed for Na and Cs concentrations with an AAS (Atomic Adsorption Spectrometry (determination limit: 0.1 and 0.2ppm for Na and Cs, respectively)). The samples for Cl were analysed with an IC (Ion Chromatography (determination limit: 0.2ppm)).

The concentration of tracer in the measurement cell becomes diluted by periodic sampling in the measurement cell and adding of groundwater to the cell. It must therefore be corrected. This was done as follows [Sato et al., in printing].

$$C_n' = C_n + \sum_{i=1}^{n-1} \frac{v_i}{V} C_i \quad (n = 2, 3, 4, \dots) \quad \text{-----} \quad (1)$$

$$C_1' = C_1 \quad (n = 1)$$

Where C_n' = the corrected concentration in the n-th sample (ppm),

C_n = the analysed concentration in the n-th sample (ppm),

V = the volume of solution in the measurement cell (m^3), and

v_i = the sample volume in the i-th sample (m^3).

2.3.2 Experiments for Se

A diffusion cell with a volume of 50ml was used in the experiments. The other specifications of the diffusion cell and rock samples are in the same as those of Na, Cs, and Cl. Since Se is a redox sensitive element, all the experiments using this element were carried out in an N₂-atmospheric glove box (O₂ < 1ppm) except for the analysis of concentration. After a rock sample was set in a diffusion cell, it was carried into the evacuation chamber of the glove box and evacuated oxygen gas existing in the rock pores by exchanging with N₂ gas. The evacuation was repeated 3 times to remove oxygen gas completely. In situ groundwater was then degassed by bubbling with atmospheric gas (N₂) in the glove box for over night. A 50ml of the degassed groundwater was then injected into both cells to saturate the rock sample. A tracer solution was prepared by dissolving an Se powder in the degassed groundwater to obtain certain concentration as shown in Table 1. At the dissolving, since the pH of the solution lowered, it was adjusted at the original pH by NaOH. After saturation of the rock, groundwater in the tracer cell was exchanged with the tracer solution, and then the experiments were initiated. Samples, 5ml, were periodically taken from the measurement cell, and an identical volume of degassed groundwater was added. Samples, 0.1ml, were taken from the tracer cell and diluted with distilled water to become 10ml. The pH, Eh and temperature of the solutions in the measurement and tracer cell were measured at every sampling. The diffusion cells were placed in the glove box during the experiments. Selenium concentrations in the sampling solutions were analysed with an ICP (Inductively Coupled Plasma) emission spectroscopy (determination limit: 0.03ppm). The correction of tracer concentration in the measurement cell was made by equation (1).

2.3.3 Experiments for HTO

The same type of diffusion cell as experiments in Se was used. The experiments were conducted in the same procedure as Na, Cs and Cl up to the saturation of groundwater. The saturation was carried out by injecting 49ml and 50ml groundwater into the tracer and measurement cell, respectively. The experiments were started by adding 1ml tritiated water

(HTO)* (0.3M Bq) into the tracer cell. Samples, 1ml, were periodically taken from the measurement cell, and an identical volume of groundwater was added. Scintillant, 4ml, was then added to each sample. Samples, 0.1ml, were also taken from the tracer cell, and scintillant was added. The concentration of HTO was counted with a liquid scintillation counter (determination limit: 3.7 Bq·ml⁻¹). The correction of tracer concentration in the measurement cell was conducted in the same way as that of Se.

2.4 Batch sorption experiments

Batch sorption experiments for Cs, Sr, Se, ²³⁸U and ²³⁹Pu were performed on fracture fillings, altered and intact granodiorite using in situ groundwater. **Table 3** shows the experimental conditions for the sorption experiments. The experiments for Cs, Sr, ²³⁸U and ²³⁹Pu were carried out under ambient aerobic conditions and those for Se were done in an N₂-atmospheric glove box (O₂ < 1ppm).

* Stock solution : 2M Bq/5ml tritiated water (provided from Amersham Japan).

Table 3 Experimental conditions for sorption experiments

Tracer	Cs	Sr	^{238}U	Se	^{239}Pu	
Concentration(initial)	$8.6 \times 10^{-5}\text{M}$	$9.13 \times 10^{-5}\text{M}$	$1.05 \times 10^{-6}\text{M}$	$1.00 \times 10^{-6}\text{M}$	$1.0 \times 10^{-4}\text{M}$	$1.55 \times 10^{-9}\text{M}$
Liquid/solid ratio	← 100ml·g ⁻¹ →		← 1000ml·g ⁻¹ →		20ml·g ⁻¹	100ml·g ⁻¹
Solid weight	← 1.0g →		← 1.5g →		0.25g	
Porewater	← in situ groundwater →					
Atmosphere	← aerobic →			← N ₂ -atmosphere (O ₂ < 1ppm) →		aerobic
Temperature	← room (23 ± 1°C) →			← room →		24°C
Experimental period	← 30 days →				← 66 days →	
Solid/liquid separation	← 0.45µm filter →			← 10000 MWCO ultrafilter →		
Producibility	← n = 3 →				← n = 2 →	

2.4.1 Sorption experiments for Cs, Sr and ^{238}U

Crushed rock powder for each rock contacted with in situ groundwater containing tracer with a liquid/solid ratio of 100 or 1000ml·g⁻¹ in a Teflon bottle and those mixtures reacted for 30 days. A blank solution without rock sample was prepared to check the decrease of concentration by sorption of tracer on the wall of the teflon bottle. The pH and Eh of all solutions were measured before the experiments. After certain period, the mixtures were filtered with a 0.45µm pore size filter and Cs and Sr concentrations in each filtered solution were measured with an AAS (Atomic Adsorption Spectrometry). The concentration of ^{238}U was measured with on ICP-MS analysis (determination limit: 4ppb). The distribution coefficients (Kd) were calculated by the following equation [Shibutani et al., 1994a].

$$Kd = \frac{C_b - C_t}{C_t} \cdot \frac{L}{S} \quad \text{-----} \quad (2)$$

Where Kd = the distribution coefficient (m³·kg⁻¹),

C_b = the tracer concentration in the blank solution (ppm),

C_t = the tracer concentration in the experimental solution (ppm),

L = the solution volume (m³), and

S = the solid weight (kg).

The error of Kd was calculated by the following equation.

$$Kde = Kd \sqrt{(E/C_t)^2 + \{2E/(C_b - C_t)\}^2} \quad \text{-----} \quad (3)$$

Where Kde = the error of Kd (m³·kg⁻¹), and

E = the error of concentration in analysis (ppm, ppb).

2.4.2 Sorption experiments for Se

All the experiments were carried out in an N₂-atmospheric glove box except for analyses. In situ groundwater was degassed by bubbling N₂ gas and added an SeO₂ powder. The groundwater containing tracer contacted with crushed rock powder with a liquid/solid ratio of 20ml·g⁻¹ in a glass bottle for 30 days. The mixtures were filtered with a 10,000 MWCO (Molecular Weight Cut-Off) ultrafilter (the pore size corresponds to 1.8nm), and the filtered solutions were analysed for Se concentrations with an ICP emission spectroscopy. The pH of the solutions was monitored as a function of time during the experiments. The distribution coefficients were calculated by equation (2). Furthermore, the specific surface areas of the samples were measured by a BET method (Flowsorb 2300, Micromeritics) using a mixture gas of 20% N₂ and 80% Ar, and those of intact and altered granodiorite and fracture fillings were 0.7, 1.9 and 1.9 m²·g⁻¹, respectively.

2.4.3 Sorption experiments for ²³⁹Pu

The experiments were carried out in the same way as Cs, Sr and U. The groundwater containing tracer contacted with crushed rock powder with a liquid / solid ratio of 100ml·g⁻¹ in a teflon bottle for 66 days. The mixtures were filtered with a 10,000 MWCO ultrafilter, and aliquots (50μl) of the filtered solutions were dried on stainless sample dishes by a hot plate. The samples were then counted for α-activity emitted from ²³⁹Pu with an α-spectrometry. The pH of the solutions was monitored as a function of time during the experiments.

2.5 CEC measurements

Cation exchange capacities (CEC) for each rock sample were measured to evaluate the cation exchangeabilities of the rock specimens, based on the Schollenberger method [JBAS, 1977]. The rock samples crushed into under 60 mesh (< 250μm) were used for the measurements. The measurements were carried out by a CEC apparatus (Fujiwara, Co. Ltd.). Powder, 0.5g, dried at 110°C for over 12hr for each rock sample was prepared. Silica sand, 5.0g, was mixed with

the dried rock powder and then was packed into a cylindrical glass column. Exchangeable cations in the rock samples were exchanged with NH_4^+ ion by flowing a 1M $\text{CH}_3\text{COONH}_4$ solution of a volume of 100ml for 7 ~ 8hr. The effluent was analysed for the concentrations of Na^+ , K^+ , Ca^{2+} , Mg^{2+} , Al, Si, Cl^- and SO_4^{2-} as leaching ions. The samples were washed by 80% ethyl alcohol for 5 ~ 6hr. The ammonium ion sorbed on the rock samples was exchanged with Na^+ by flowing a 10% NaCl solution for 7 ~ 8hr. The effluent was added 100ml distilled water and a 50ml of 50% NaOH and was then heated by a mantel heater. A 20ml of 0.05N sulfuric acid (H_2SO_4) and 2ml pH indicator which a 0.2% methyl red ($\text{C}_{15}\text{H}_{15}\text{N}_3\text{O}_2$) alcohol and a 0.1% bromcresol green ($\text{C}_{21}\text{H}_{14}\text{Br}_4\text{O}_5\text{S}$) alcohol solution were mixed at a volume ratio of 2 to 3, were added to the solution. The solution was then titrated by 0.02N NaOH. Cation exchange capacity per 100g sample weight was calculated by the following equation.

$$CEC = \frac{(A-B) \cdot f \cdot 2}{W \cdot \frac{100-M}{100}} \text{-----} (4)$$

Where CEC = the cation exchange capacity (meq/100g)

A = the volume of 0.02N NaOH used for titration in blank (ml),

B = the volume of 0.02N NaOH used for titration (ml),

f = the concentration factor of 0.02N NaOH (-),

M = the water content of the sample (wt%), and

W = the sample weight under air (g).

2.6 Measurements of porosity and pore-size distribution in rock matrix

Porosity and density of each rock sample were determined by both a water saturation method and a mercury porosimetry, and pore-size distribution and specific surface area of pores were measured by the mercury porosimetry.

2.6.1 Water saturation method

The porosity was determined from the difference between the dry and saturated sample weight. The water density is approximately $1.0 \times 10^3 \text{ kg}\cdot\text{m}^{-3}$, making the pore volume of the rocks equal to the weight of the water.

A rock sample was immersed in distilled water and put in a vacuum vessel, then soaked under about 30 torr pressure condition. The sample was periodically taken out and the water wiped off its surface, then weighed. This operation was repeated until the sample weight reached a constant value. After saturation, the volume of the saturated sample was measured by the difference between the water levels in a measuring cylinder. Then, the sample was dried at 110°C in an oven until the weight reached a constant value. The porosity was calculated as the ratio of the weight difference between the water-saturated and dried rock sample to the total sample volume [Monicard, 1980]. The porosity was determined by the following equation:

$$\varepsilon = \frac{M_1 - M_2}{\rho_w \cdot V_r} \text{-----} (5)$$

Where ε = the porosity (-),

M_1 = the weight of the water-saturated rock sample (kg),

M_2 = the weight of the dried rock sample (kg),

V_r = the total volume of the rock sample (m^3), and

ρ_w = the density of distilled water ($\text{kg}\cdot\text{m}^{-3}$).

2.6.2 Mercury porosimetry

Mercury has a contact angle of $90 \sim 180^\circ$ for almost all materials. The mercury is impregnated by force, the relationship between the applied pressure and the size of the pores into which it enters is determined by the balance between the surface tension of mercury and the applied pressure to mercury. The pore-size distribution, porosity, specific surface area of the pores and dry density were measured by this method. A mercury porosimeter (Autopore 9200, Shimadzu) was used in the measurements. Mercury porosimetry is based on capillary action.

For a non-wetting liquid such as mercury, the relationship between the cylindrical pore size and applied pressure is given by Washburn's law.

$$D = -\frac{4}{P} \gamma \cdot \cos \theta \text{ ----- (6)}$$

Where D = the pore diameter (m),

P = the pressure applied to mercury (N·m⁻²),

γ = the surface tension (N·m⁻¹), and

θ = the contact angle (°).

The surface tension, γ = 0.484 N·m⁻¹ and the contact angle, θ = 130° for mercury to common soil have been adopted in general. In these measurements, pores up to minimum pore size 3.4nm were measured. Based on equation (6), the pore-size distribution was derived from the applied pressure.

A 1cm-sized block sample was used for the measurements. The measurements were continuously and automatically made, and those done in triplicate.

In actual measurement, mercury volume entered the pores of rock was directly monitored as a function of applied pressure, then converted to pore sizes based on equation (6). The pore-size distribution stands for an accumulated pore volume per unit sample weight as a function of pore size, and a specific pore volume means a pore volume per unit sample weight. Furthermore, a specific surface area of the pores was derived from the measurement based on the cylindrical pore model (tube model). The specific surface area of the pores is derived by the following equation.

$$S_p = -\frac{1}{\gamma \cdot \cos \theta} \int_{V_{min}}^{V_{max}} P dx \text{ ----- (7)}$$

Where Sp = the specific surface area of the pores (m²·kg⁻¹),

Vmax = the mercury volume in the cell when mercury is injected to maximum pore size (m³),

and

V_{min} = the mercury volume in the cell when mercury is injected to minimum pore size (m^3).

The dry density of the sample is calculated by the following equation.

$$\rho_d = \frac{Mr}{v - \frac{W_m}{\rho_m}} \quad \text{-----} \quad (8)$$

Where ρ_d = the dry density of the sample ($m^3 \cdot kg^{-1}$),

Mr = the sample weight (kg),

v = the cell volume to put the sample in (m^3),

W_m = the mercury weight (kg), and

ρ_m = the mercury density ($13.6 \text{ kg} \cdot \text{dm}^{-3}$).

The porosity is calculated by the following equation as the product of specific pore volume and dry density of the sample.

$$\varepsilon = V_s \cdot \rho_d \quad \text{-----} \quad (9)$$

Where ε = the porosity (-), and

V_s = the specific pore volume ($m^3 \cdot kg^{-1}$).

3. RESULTS

3.1 Diffusion coefficients

Figure 4 shows examples of the changes in concentration of Cs in the measurement cell as a function of time for each rock sample. The concentration of Cs in the measurement cell shows a curve in transient state and increases in a straight line with time in steady state. Similar behaviour was also found in the other rocks. The differences in slope between the changes in concentration with time for each rock are found. These differences directly stand for the

differences in D_e . Tracer concentration in the tracer cell is essential for calculation of D_e . In this study, the concentration of tracer in the tracer cell was monitored and the significant decrease was not found. Moreover, no sorption on the wall of the cell was found. Therefore, the final tracer concentration was used in the computation of the D_e . The calculations of D_e and D_a were based on Fick's law [Crank, 1975]. Diffusion equation for one-dimension is generally expressed by the following equation on the basis of Fick's second law [Skagius and Neretnieks, 1982].

$$\frac{\partial C_p}{\partial t} = \frac{\varepsilon \cdot D_p}{\alpha} \cdot \frac{\partial^2 C_p}{\partial X^2} \text{-----} (10)$$

Where C_p = the concentration of tracer in the porewater (ppm),

t = the diffusing time (s),

D_p = the diffusion coefficient in the porewater ($m^2 \cdot s^{-1}$),

α = the rock capacity factor ($\alpha = \varepsilon + \rho \cdot K_d$),

ε = the porosity (-),

ρ = the dry density of the rock sample ($kg \cdot m^{-3}$),

K_d = the distribution coefficient ($m^3 \cdot kg^{-1}$), and

X = the distance from the source in the diffusing direction (m).

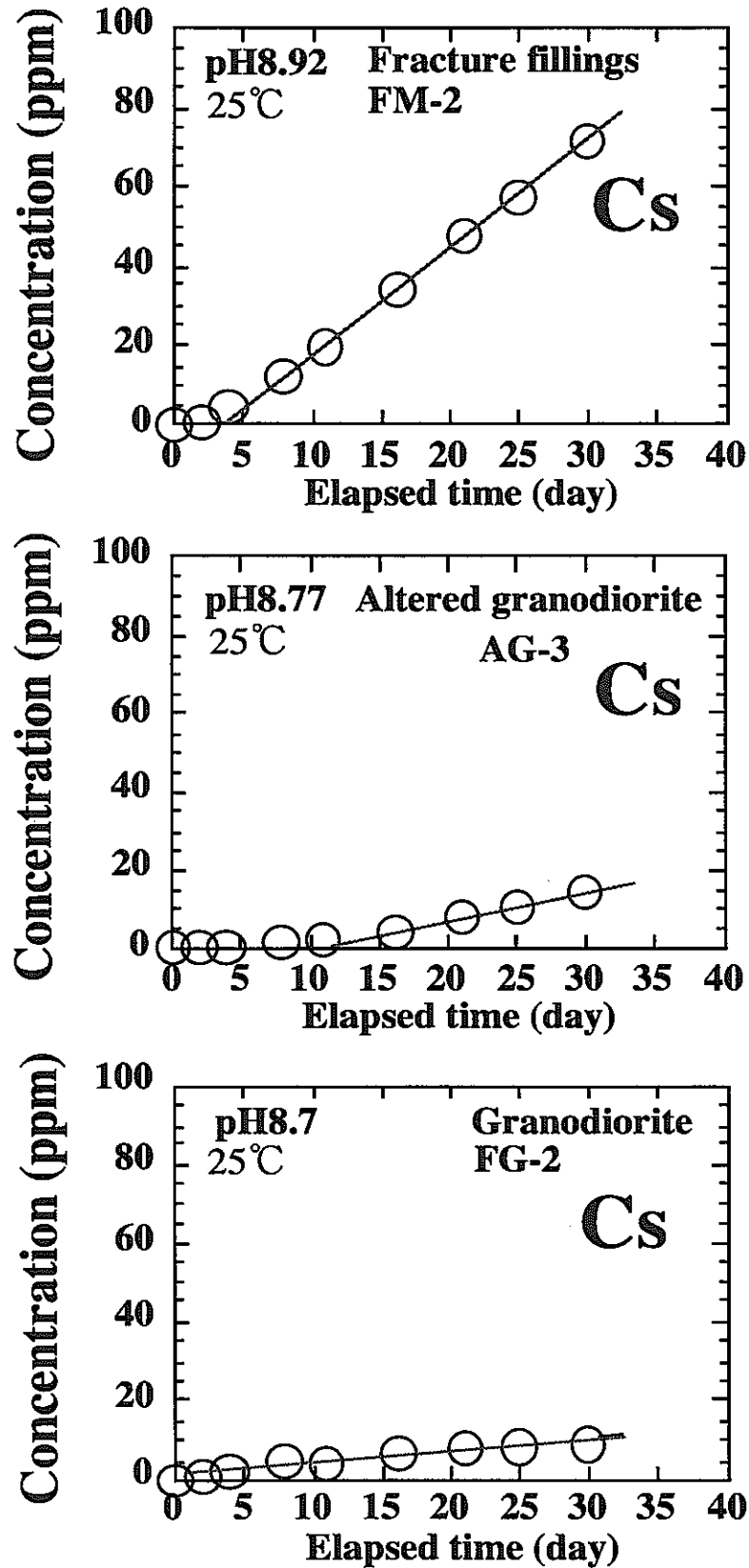


Figure 4 Changes in concentration of Cs in the measurement cell as a function of time for fracture fillings, altered and intact granodiorite

The $\epsilon \cdot D_p$ is also called effective diffusion coefficient (De). Moreover, the $\epsilon \cdot D_p / \alpha$ is equal to apparent diffusion coefficient (Da). For equation (10), the concentration of tracer in the measurement cell at an arbitrary time, based on initial and boundary conditions, is written as follows [Crank, 1975]:

Initial condition

$$C_p(t, X) = 0, t = 0, 0 \leq X \leq H$$

Boundary condition

$$C_p(t, X) = C_0, t > 0, X = 0$$

$$C_p(t, X) = 0, t > 0, X = H$$

$$C_t = \frac{S_r \cdot H \cdot C_0}{V_m} \left[\frac{De}{H^2} t - \frac{\alpha}{6} - \frac{2\alpha}{\pi^2} \sum_{n=1}^{\infty} \left\{ \frac{(-1)^n}{n^2} \exp\left(-\frac{De \cdot n^2 \cdot \pi^2 \cdot t}{H^2 \cdot \alpha} \right) \right\} \right] \dots\dots\dots (11)$$

In the actual experiment, Cp in the measurement cell increased as a function of time. However, the increase in Cp was so small that it is able to be neglected compared with the concentration (Co) of tracer in the tracer cell. Equation (11) is approximately written for steady state as follows [Crank, 1975]:

$$C_t = \frac{S_r \cdot H \cdot C_0}{V_m} \left(\frac{De}{H^2} t - \frac{\alpha}{6} \right) \dots\dots\dots (12)$$

- where H = the thickness of the sample (m),
- C0 = the concentration of tracer in the tracer cell (ppm),
- Ct = the concentration of tracer in the measurement cell (ppm),
- Sr = the cross-section area of the sample (m²),
- Vm = the volume of the solution in the measurement and tracer cell (m³), and
- α = the rock capacity factor (-).

Effective diffusion coefficient was calculated from the slope of C_t as a function of time in steady state based on equation (12). Furthermore, D_a was calculated by the time-lag method [Muurinen et al., 1987] which relationship is given by the following equation.

$$D_a = \frac{H^2}{6T_{int}} \text{-----} (13)$$

Where T_{int} = the intercept on the t-axis extrapolated by equation (11),

D_a = the apparent diffusion coefficient ($m^2 \cdot s^{-1}$), and

H = the thickness of the sample (m).

Table 4 shows average D_e and D_a values and rock capacity factors estimated for each element. The average pH values are also shown in **Table 4**. The initial pH of groundwater was about 9.3, and those for Na, Cs, HTO and Cl gradually decreased as a function of time and became at pH about 8.0, 8.3 and 8.5 for intact and altered granodiorite and fracture fillings, respectively after 30 days. On the contrary, no pH changes for Se in experiments conducted under anaerobic conditions were observed, and the pH values remained at 9.3. These differences of pH values are considered to be due to dissolution of carbon dioxide ($CO_2 + H_2O = HCO_3^- + H^+$) in the former experiments. The effective diffusion coefficients for all elements showed a tendency of fracture fillings > altered granodiorite > intact granodiorite. On the other hand, for the D_a values, remarkable difference in kind of the rock was not found.

For the change in temperature of the experiments, the experiments for Na, Cs and Cl were carried out in a thermobath kept at 25°C, but those only for Se were carried out in a glove box being monitored. The temperature ranged from 18 to 23°C and the average was approximately 22°C. The variation in temperature was not so large. The experiments for HTO were conducted at room temperature (23°C).

Table 4 Average apparent and effective diffusion coefficients estimated for each ion

Rock	Ion	Da (m ² ·s ⁻¹)	De (m ² ·s ⁻¹)	α (-)	pH
Intact granodiorite	Na ⁺	4.3x10 ⁻¹¹	4.7x10 ⁻¹²	0.11	8.7
	Cs ⁺	1.1x10 ⁻¹¹	5.1x10 ⁻¹²	0.46	8.7
	HTO	2.1x10 ⁻¹⁰	5.3x10 ⁻¹²	0.025	8.7
	Cl ⁻	9.8x10 ⁻¹²	1.0x10 ⁻¹¹	1.0	8.7
	SeO ₃ ²⁻	6.5x10 ⁻¹²	1.9x10 ⁻¹²	0.29	9.29
Altered granodiorite	Na ⁺	9.7x10 ⁻¹²	7.2x10 ⁻¹²	0.74	8.77
	Cs ⁺	4.5x10 ⁻¹²	1.2x10 ⁻¹¹	0.27	8.77
	HTO	5.6x10 ⁻¹⁰	1.8x10 ⁻¹¹	0.032	8.7
	Cl ⁻	1.0x10 ⁻¹¹	8.3x10 ⁻¹²	0.83	8.77
	SeO ₃ ²⁻	1.1x10 ⁻¹¹	2.9x10 ⁻¹²	0.26	9.33
Fracture fillings	Na ⁺	2.0x10 ⁻¹¹	1.9x10 ⁻¹¹	0.95	8.92
	Cs ⁺	1.2x10 ⁻¹¹	1.8x10 ⁻¹¹	1.5	8.92
	HTO	4.3x10 ⁻¹⁰	2.4x10 ⁻¹¹	0.056	8.92
	Cl ⁻	2.6x10 ⁻¹¹	1.8x10 ⁻¹¹	0.69	8.77
	SeO ₃ ²⁻	5.9x10 ⁻¹²	5.3x10 ⁻¹²	0.90	9.53

3.2 Distribution coefficients

Table 5 shows the experimental results for the sorptions of Cs, Sr, Se, ^{238}U and ^{239}Pu . The distribution coefficients of Cs and Sr were in the order; fracture fillings > intact granodiorite \geq altered granodiorite. Though those of Se showed a tendency of fracture fillings > altered granodiorite \geq intact granodiorite, all the values were quite low and approximately the same extent. Sorption mechanisms for these elements will be discussed in detail together with the measurements of CEC values of the rocks in the part of discussion. A liquid / solid ratio dependence was found in U sorption, and U hardly sorbed for a liquid / solid ratio of $100\text{ml}\cdot\text{g}^{-1}$, but significant sorptions were recognized for a liquid / solid ratio of $1000\text{ml}\cdot\text{g}^{-1}$. The distribution coefficients are in the order of fracture fillings > altered granodiorite > intact granodiorite. The sorption property of Pu showed the reverse order compared with that in U.

Table 5 Experimental results for sorption

Rock	Cs		Sr		Se		238U		239Pu			
	solid/liquid ratio($\text{ml}\cdot\text{g}^{-1}$)											
							100		1000			
	pH*	Kd ($\text{ml}\cdot\text{g}^{-1}$)	pH*	Kd ($\text{ml}\cdot\text{g}^{-1}$)	pH*	Kd ($\text{ml}\cdot\text{g}^{-1}$)	pH*	Kd ($\text{ml}\cdot\text{g}^{-1}$)	pH*	Kd ($\text{ml}\cdot\text{g}^{-1}$)		
Intact granodiorite		28 \pm 1		27 \pm 2	9.27	0.00		0 \pm 2		12 \pm 16	8.04	3230
	9.38	29 \pm 1	9.43	38 \pm 2	9.32 (9.30)**	0.94	8.42	4 \pm 2	9.45	25 \pm 16	~	5210
		29 \pm 1		44 \pm 2	9.31	0.62		9 \pm 2		25 \pm 16	9.16	
Altered granodiorite		17 \pm 1		36 \pm 2	9.36	0.30		0 \pm 2		51 \pm 17	8.04	3230
	9.48	18 \pm 1	9.45	36 \pm 2	9.37 (9.37)**	0.94	8.65	0 \pm 2	9.46	51 \pm 17	~	2560
		18 \pm 1		36 \pm 2	9.40	1.61		0 \pm 2		69 \pm 17	9.16	
Fracture fillings		96 \pm 2		48 \pm 2	9.28	0.62		3 \pm 2		38 \pm 17	8.04	1770
	9.44	107 \pm 2	9.42	50 \pm 2	9.28 (9.29)**	1.27	8.88	3 \pm 2	9.48	83 \pm 17	~	1360
		111 \pm 2		53 \pm 2	9.30	1.61		6 \pm 2		142 \pm 17	9.16	

* The pH shows the values after 30 days.

** The number in () stands for average value.

*** The pH shows the values after 66 days.

3.3 CEC values of the rock specimens

Table 6 shows the results of CEC measurements and leaching ions for each rock sample. For intact and altered granodiorite, slight CEC values (about 2 meq/100g) were obtained, and those for fracture fillings and mixture of each rock (sample from fracture type C) were measured to be about 17 and 62 meq/100g, respectively. The cause that the CEC values of fracture fillings and mixture of each rock were higher than other rock matrix, is considered to be due to constituent stilbite which has a high CEC. In all the cases, not so much CEC values except for mixture of each rock were measured. For leaching ions, amount of Ca^{2+} in effluent was outstandingly the highest of the analysed ions for all the rocks, and the leached quantities of Ca^{2+} were in the order of fracture fillings > altered granodiorite > intact granodiorite. This could be caused by dissolution of calcite and stilbite contained in the fracture fillings. There is a possibility that the CEC of rock gives an influence to K_d of an ion exchangeable element. In this study, batch sorption experiments for Cs and Sr as an ion exchangeable elements were carried out. Relation between CEC values of the rocks and K_d values of Cs and Sr will be discussed in the part of discussion.

Table 6 The CEC and leaching ions

	meq/100g			
Ion	Intact granodiorite*	Altered granodiorite*	Fracture fillings*	Sample from fracture type C*
Na ⁺	26.0	84.0	217.3	1023.0
K ⁺	15.3	25.5	25.5	61.3
Ca ²⁺	475.6	3179.2	23874.7	6613.2
Mg ²⁺	16.4	32.9	32.8	65.8
Al ^{**}	< 0.15	< 0.15	< 0.15	< 0.15
Si ^{**}	5.3	6.5	45.1	35.6
Cl ⁻	15.0	82.7	< 0.11	26.3
SO ₄ ²⁻	< 0.17	16.6	< 0.17	23.5***
CEC	2.0	1.9	17.3	61.2

* The number stands for average value.

** The unit for Al and Si is mmol/100g.

*** The two samples of three samples are below the detection limit (< 0.11 meq/100g).

3.4 Porosity and pore-size distribution in rock

Table 7 shows the results for the porosity, specific surface area of pores and dry density obtained by both water saturation method and mercury porosimetry. **Figure 5** shows a correlation between porosity and rock samples. Though some variations in porosity are found, the average porosities were in the order; fracture fillings (5.6%) > altered granodiorite (3.2%) > intact granodiorite (2.3%). Relatively large variation in the porosity of fracture fillings measured by water saturation method was found. This reason is considered to be due to that the samples used for the measurements were small. From this fact, it was cleared that porosity became small into the rock matrix from the fracture. Porosity of intact granodiorite has been reported to be around 1% [Suzuki et al., 1989]. The authors have measured the porosities to be 1.2% on the average by the same ways for granodiorite sampled from different area [Sato et al., in printing], and the porosities (average 2.3%) measured for intact granodiorite in this study were a little higher than those. However, the porosities in this study are approximately the same as those of common granodiorite.

Figure 6 shows examples in pore-size distribution measured for each rock. The pore sizes of intact granodiorite are in the range of 10nm ~ 0.2mm, and no pores smaller than 10nm were measured. Nishiyama et al. [1990] have reported similar results for the pore-size distribution of granite (sampled from Inada, Japan) measured by the same way. Similar results have been also obtained for altered granodiorite. The difference in porosity between intact and altered granodiorite is due to that the frequency of pore sizes between 0.1 μ m and 10 μ m in altered granodiorite is more than that of intact granodiorite, and this indicates that pores in this range increased by alteration. Fracture fillings have a pore-size distribution of 50nm to 0.2mm and show a variety of unevenly distributed pore sizes, i.e. a lot of pores have been found around 0.1 μ m and 0.2mm in the fracture fillings. From these pore-size distributions, it was cleared that relatively large pore sizes were predominant compared with ionic sizes.

Table 7 Porosities, dry densities and specific surface area of pores for each rock

Rock	Method	Specific surface area (m ² ·g ⁻¹)	Dry density (kg·m ⁻³)	Porosity (%)	Porosity (average)
Intact granodiorite	Mercury	0.6	2700	3.0	2.3
		0.2	2700 (2730)	2.4 (2.8)	
		0.5	2800	3.0	
	Water		2610	2.8	
			2770 (2730)	1.2 (1.7)	
			2700	1.7	
Altered granodiorite	Mercury	0.6	2600	2.3	3.2
		0.6	2600 (2600)	3.4 (3.2)	
		0.6	2600	3.9	
	Water		2620	3.3	
			2580 (2620)	3.3 (3.3)	
			2650	3.2	
Fracture fillings	Mercury	0.4	2500	3.8	5.6
		0.7	2400 (2460)	4.3 (4.5)	
		0.4	2400	5.3	
	Water		2350	7.4	
			2840 (2410)	3.7 (6.6)	
			2180	5.8	
		2260	9.6		

* (): average value

** Mercury and Water mean mercury porosimetry and water saturation method, respectively

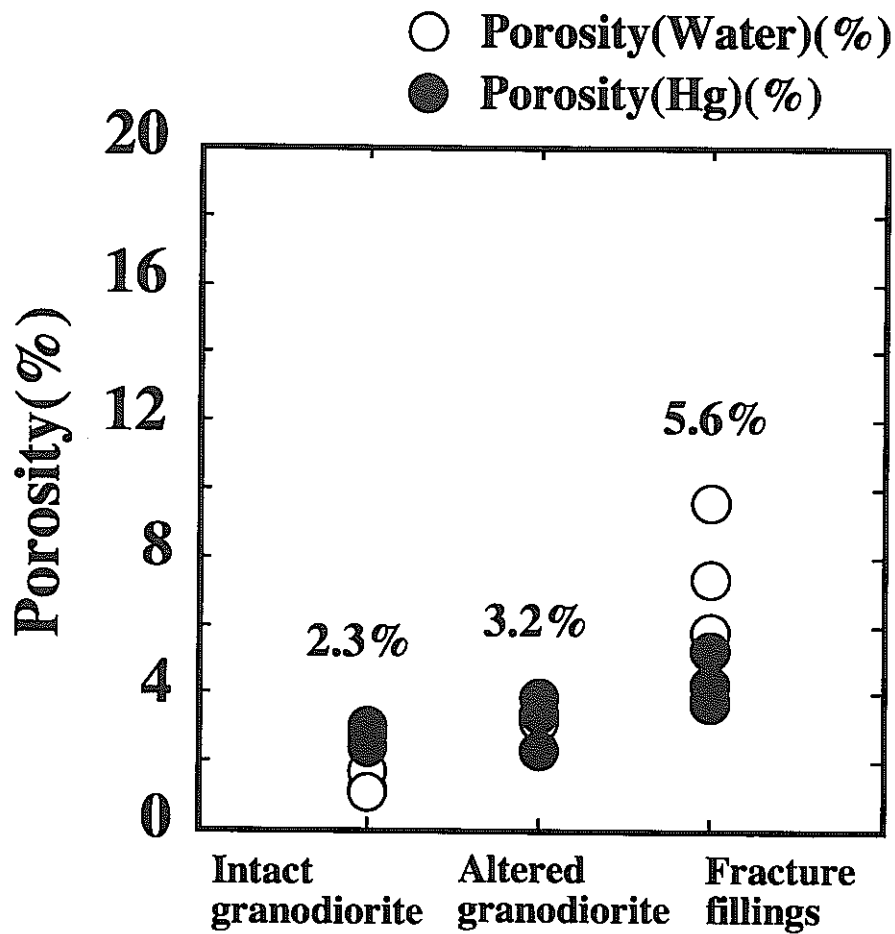


Figure 5 Correlation between porosity and rock sample

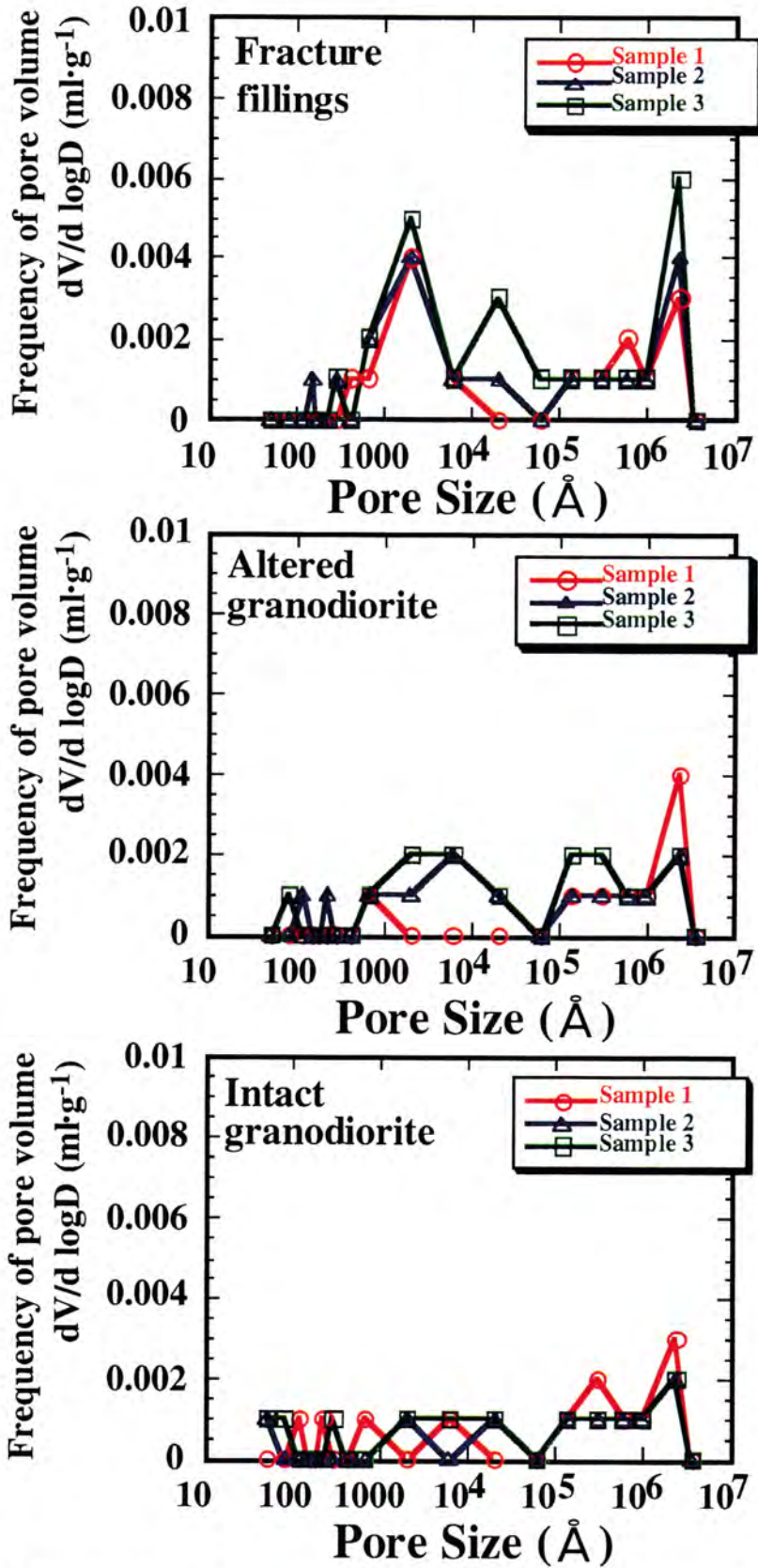


Figure 6 Examples of measurement in pore-size distribution by mercury porosimetry for each rock. Each graph shows frequency as a function of pore diameter.

4. DISCUSSION

4.1 Relations between diffusion coefficients and porosities

Figures 7 and 8 show D_e and D_a values as a function of porosity, respectively. The average porosities of each rock sample measured by both water saturation method and mercury porosimetry were used as these porosities. For Na, Cs and Cl, the data on standard granite [Sato et al., in printing; Sato and Shibutani, 1996] are also plotted together. The effective diffusion coefficients for all species showed a tendency of decrease with decreasing the rock porosity, and no significant difference between species in the D_e values was observed. Namely, the D_e values approximately correspond to porosity. The dominant species of Na, Cs, Cl and Se in the porewater in the pH range of this study are predicted to be Na^+ , Cs^+ , Cl^- and SeO_3^{2-} from Eh-pH diagrams [Brookins, 1988], respectively. Since HTO is a part of water molecule, it is able to be regarded as neutral species. Therefore, the electrostatic interaction with the rock pore surface in HTO is able to be neglected. Since the other species are charged, electrostatic interactions with the rock pore surface are presumed to occur. However, the effect of ionic charge on D_e was not so significant, as described above. Yamaguchi et al. [1992] have experimentally studied the surface diffusion of Sr^{2+} in granite (Inada, Japan) by through-diffusion method. In this work, they measured D_e values of Sr^{2+} as a function of the ionic strength of porewater (0.1M KCl (pH=4.0) and deionized water) and explained the diffusion behaviour of Sr^{2+} taking into account surface diffusion from relation between rock capacity factor and the ionic strength of porewater. From these experiments, relatively high D_e values ($1 \sim 2 \times 10^{-11} \text{ m}^2 \cdot \text{s}^{-1}$) for deionized water were measured compared with those ($1.8 \sim 3.2 \times 10^{-13} \text{ m}^2 \cdot \text{s}^{-1}$) for 0.1M KCl. However, the breakthrough curves for deionized water have large variation and are unclear slope for the calculation of D_e . Since neither pore-size distribution in this rock nor porosity is described, electrostatic interaction with the rock pore surface is unclear. After that, Yamaguchi et al. [1996] have reported on the measurements of porosity and pore-size distribution in granite by both a water saturation method and a mercury porosimetry, respectively. In this work, the porosity has been reported to be $0.49 \pm 0.06\%$ and 0.47% on the average by water saturation method and mercury porosimetry, respectively. Furthermore, the

pore-size distribution has been reported to be in the range of 25 ~ 1000nm and relatively large pores compared with ionic sizes. Also in our study, in the measurements of pore-size distribution in the rocks by mercury porosimetry, no pores smaller than 10nm for all the rock samples were measured, and relatively large pores from the viewpoint of ionic diffusion were predominant. This means that the pore sizes are much larger than ionic sizes and the effect of electrostatic interaction of diffusion species with the rock pore surface is not significant. Therefore, it is considered that diffusion in the porewater becomes dominantly in these rock matrixes.

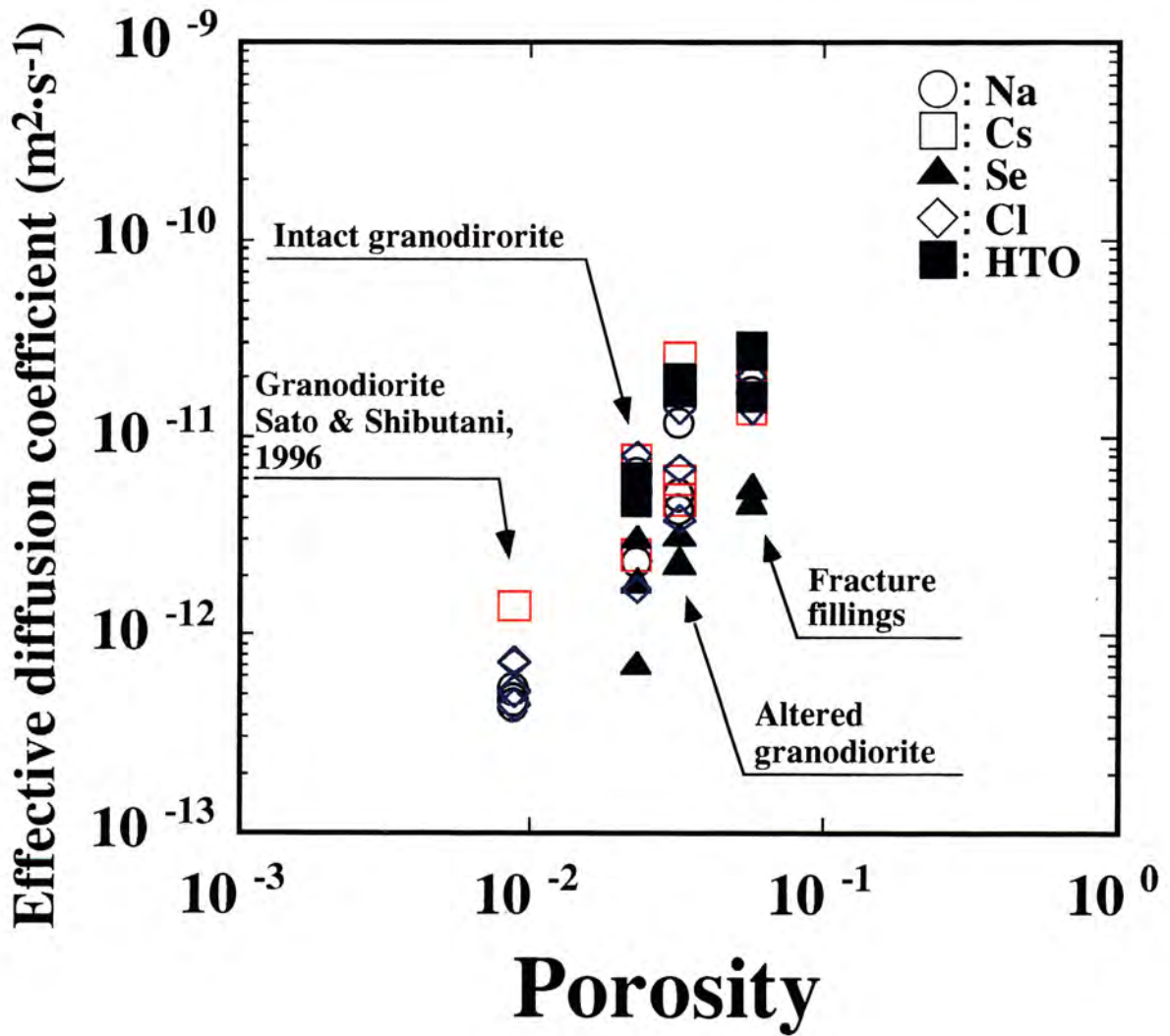


Figure 7 Effective diffusion coefficients as a function of porosity

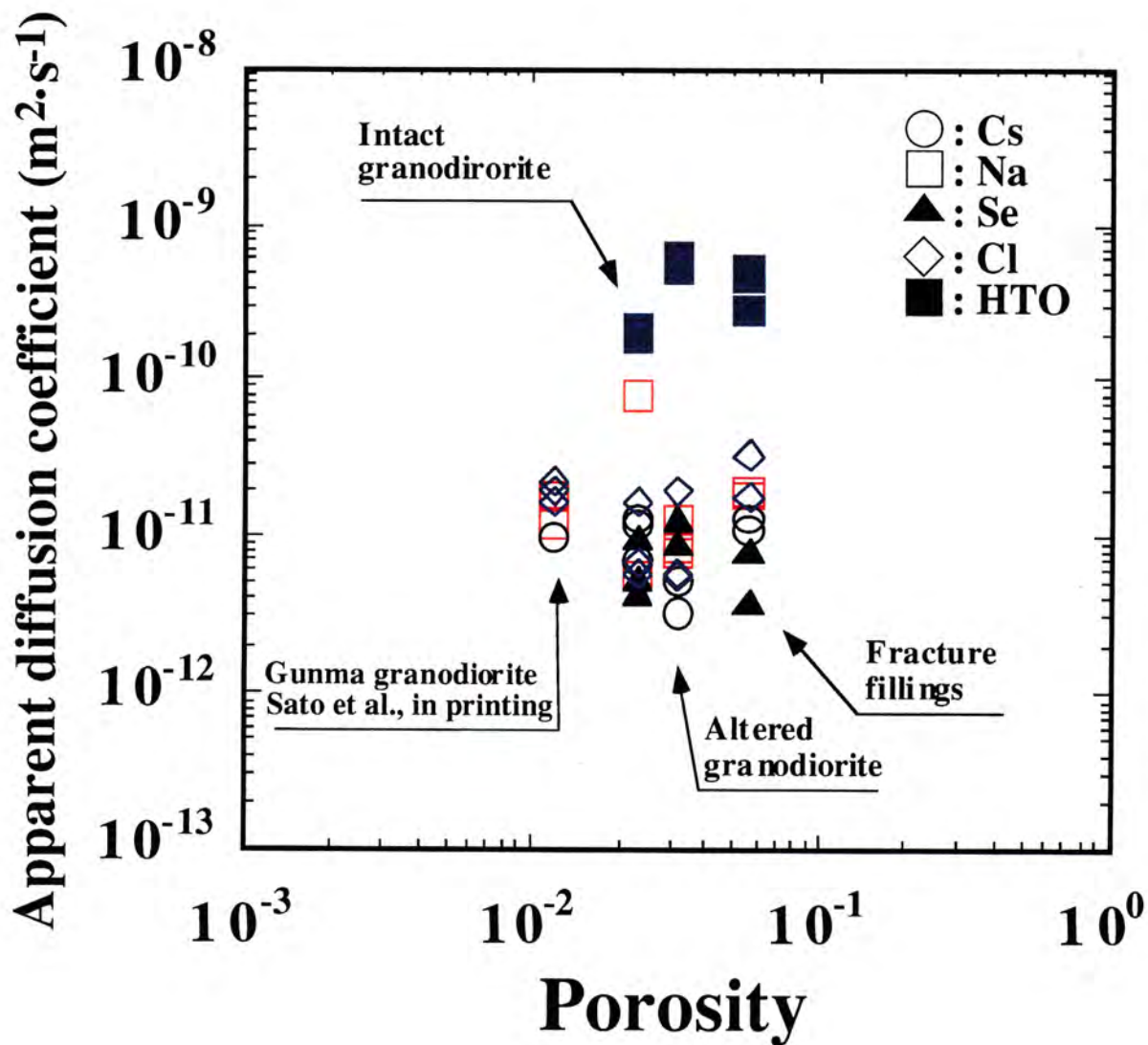


Figure 8 Apparent diffusion coefficients as a function of porosity

Effective diffusion coefficient is disintegrated as follows.

$$De = \varepsilon \cdot \frac{\delta}{\tau^2} \cdot Dv = \varepsilon \cdot G \cdot Dv = FF \cdot Dv \text{ ----- (14)}$$

where ε = the porosity (-),

δ = the constrictivity (-),

τ^2 = the tortuosity (-),

Dv = the ionic diffusion coefficient in free water ($m^2 \cdot s^{-1}$),

G = the geometric factor (or tortuosity factor) (-), and

FF = the formation factor (-).

As shown by equation (14), there is a possibility that De is also affected by porosity, geometric factor, which expresses the rock pore structure and ionic diffusion coefficient in free water. Therefore, it is not able to be simply evaluated, by which parameter the De is mainly affected. The geometric factor was calculated based on equation (14) to evaluate the effect of the rock pore structure. The geometric factor is calculated by the following equation modifying equation (14).

$$G = \frac{De}{\varepsilon \cdot Dv} \text{ ----- (15)}$$

The ionic diffusion coefficient in free water is calculated by the Nernst expression [Robinson and Stokes, 1959; Shackelford and Daniel, 1991; Daniel and Shackelford, 1988].

$$Dv = \frac{R \cdot T \cdot \lambda}{F^2 \cdot |Z|} \text{ ----- (16)}$$

Where Dv = the ionic diffusion coefficient in free water ($m^2 \cdot s^{-1}$),

R = the gas constant ($8.314 \text{ J} \cdot \text{mol}^{-1} \cdot \text{K}^{-1}$),

T = the absolute temperature (K),

λ = the limiting ionic equivalent conductivity ($m^2 \cdot S \cdot \text{mol}^{-1}$),

F = the Faraday constant ($96,493 \text{ C}\cdot\text{mol}^{-1}$), and
 $|Z|$ = the absolute value of the ionic charge (-).

The ionic diffusion coefficients in free water of Na^+ , Cs^+ , Cl^- and SeO_3^{2-} are calculated to be 1.33×10^{-9} , 2.05×10^{-9} , 2.03×10^{-9} and $9.6 \times 10^{-10} \text{ m}^2\cdot\text{s}^{-1}$ at 25°C [Kagaku-binran, 1975], respectively by substituting their limiting ionic equivalent conductivities into the Nernst expression in this study. The limiting ionic equivalent conductivity of HTO has not been measured because it is a neutral species, but directly measured its self-diffusion coefficient has been reported to be $2.14 \times 10^{-9} \text{ m}^2\cdot\text{s}^{-1}$ at 25°C [Kagaku-binran, 1975].

Figure 9 shows the calculated results in the geometric factors (G) as a function of porosity. As **Figure 9** shows, though some variations are recognized depending on species, all the G values are approximately the same (G : about 0.1) without depending on the rock porosity. From this fact, it can be seen that porosity dependence of D_e is not caused by the dependence of G on porosity, but is caused by that of formation factor which is the product of porosity and G .

The formation factor is also calculated by equation (14). Since D_e depends on D_v , formation factors for each rock were calculated to check, by which parameter the D_e is mainly affected. **Figure 10** shows the calculated results in the formation factors of the rocks as a function of porosity. As **Figure 10** shows, the formation factors for all the species significantly decrease with decreasing the rock porosity. Even though the G is approximately constant without depending on the rock porosity, a porosity dependence is found in the formation factors. Therefore, it is concluded that though D_e is determined by porosity, geometric factor and D_v , the degree of porosity dependence in D_e is affected by only porosity.

Though D_e values are dependent on the rock porosity as described above, no remarkable dependence on the rock porosity in D_a values is found, and neither is large variation in the D_a values found except for HTO. Since HTO is a non-sorbing nuclide, it is presumed that the D_a values of HTO were about one order of magnitude higher than those of other species.

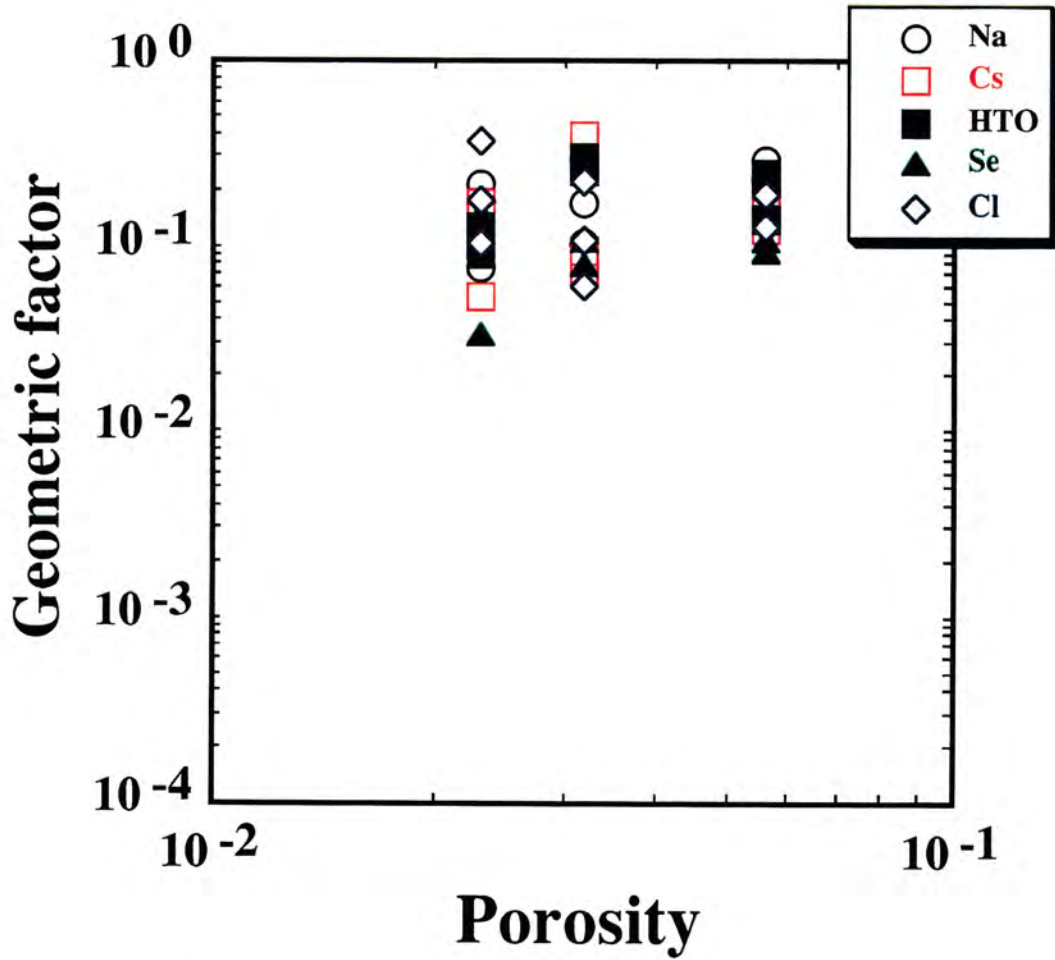


Figure 9 Geometric factor as a function of porosity

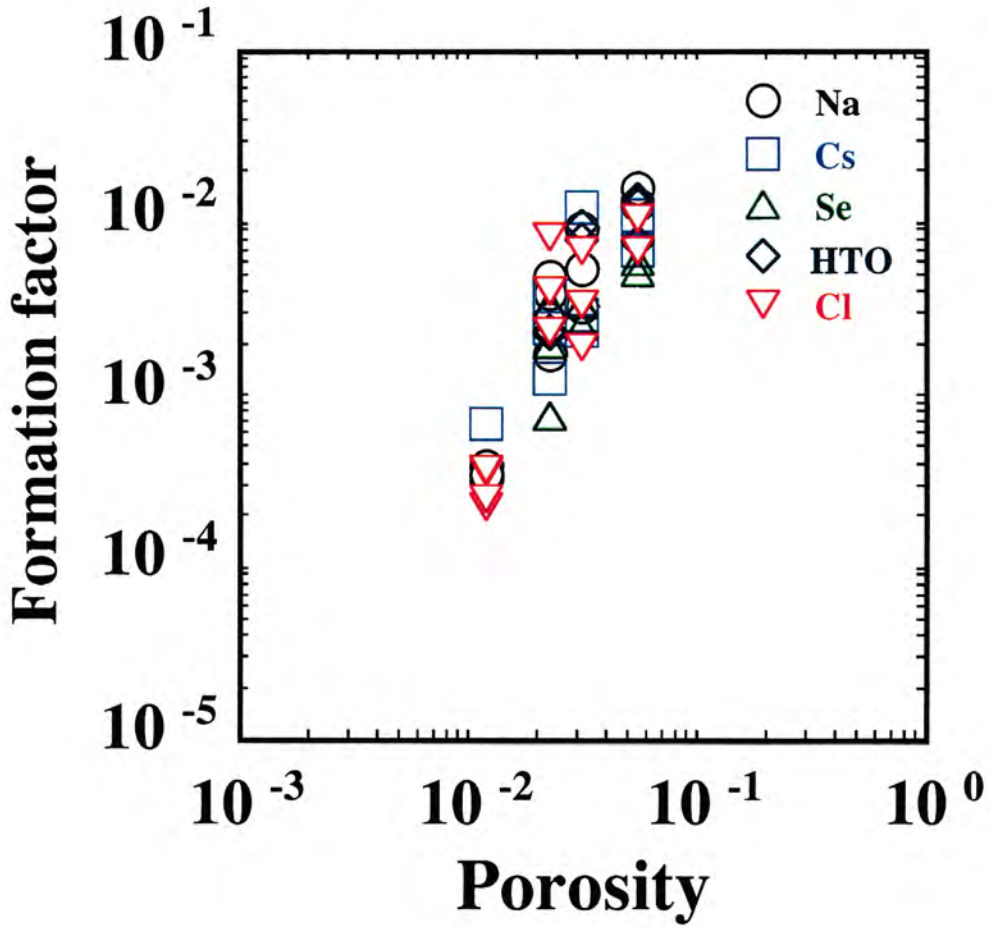


Figure 10 Formation factors of the rocks as a function of porosity

Distribution coefficients of Cs and Se on each rock were calculated from rock capacity factors, density and porosities, and compared with those obtained from batch sorption experiments. **Table 8** shows the calculated results and the comparison. All the Kd values in Cs and Se obtained from diffusion experiments are lower than those obtained from batch sorption experiments. In comparison between specific surface areas of the rock samples, the specific surface areas of samples used in batch sorption experiments are higher than those of samples used in diffusion experiments. Since sorption occurs on the rock surface, the specific surface areas of pores in the Kd values obtained from diffusion experiments were converted to those of crushed rocks used in batch sorption experiments. Consequently, the converted Kd values for Se are relatively consistent with those obtained from batch experiments, but the converted Kd values for Cs are one order of magnitude or more higher than those obtained from batch experiments. A concentration dependence of Cs in Kd on the rock is possible in this case. Sorption and diffusion experiments for Se were conducted by tracers with approximately the same concentrations, but those for Cs were carried out using tracers with largely different concentrations, i.e. tracer concentration of Cs used in diffusion experiments is two orders of magnitude or more higher than that used in batch sorption experiments. Consideration for isotherm of Cs in Kd on the rock is required to evaluate concentration dependence in sorption.

Table 8 Comparison between distribution coefficients obtained from both diffusion and batch sorption experiments

Rock	Element (nuclide)	Diffusion		Batch method	
		pH	Kd (ml·g⁻¹)	pH	Kd (ml·g⁻¹)
Intact granodiorite	Cs⁺	8.7	0.18	9.38	28.7
	SeO₃²⁻	9.29	0.1	9.30	0.52
Altered granodiorite	Cs⁺	8.77	0.35	9.48	17.7
	SeO₃²⁻	9.33	0.09	9.37	0.95
Fracture fillings	Cs⁺	8.92	0.60	9.44	104.7
	SeO₃²⁻	9.53	0.40	9.29	1.2

4.2 Relation between Kd and CEC values

In the measurements of CEC for intact and altered granodiorite, approximately the same CEC values (about 2 meq/100g) were obtained, and those of fracture fillings and mixture of each rock (fracture type C) were measured to be about 17 and 62 meq/100g, respectively. The dominant species for each element under studied conditions are predicted to be Cs^+ , Sr^{2+} , SeO_3^{2-} , $\text{UO}_2(\text{CO}_3)_3^{4-}$ and $\text{Pu}(\text{CO}_3)_3^{2-}$. Cesium and strontium are generally said to sorb on geological materials by ion exchange. Relation between Kd values of Cs and Sr and CEC values for each rock was discussed. Distribution coefficients of Cs and Sr obtained from batch sorption experiments were in the order of fracture fillings > intact granodiorite \geq altered granodiorite and the trend is relatively consistent with that of CEC. The dominant sorption mechanism of Cs and Sr on the rock matrix could be ion exchange from this. However, the Kd values of Cs on the altered granodiorite are about two thirds of those on the intact granodiorite. This probable reason is that amount of competing ions such as Na^+ , K^+ , Ca^{2+} and Mg^{2+} in sorption experiments on the altered granodiorite was much more than that in sorption experiments on the intact granodiorite, as shown in **Table 6**.

On the contrary, Se is known to show different sorption behaviour from that of Cs and Sr. Shibutani et al. [Shibutani et al., 1994b] have reported sorptions for Se on various rocks and their constituent minerals as a function of pH by batch method under anaerobic conditions. From these results, slight sorption on granodiorite is shown in the wide pH range (5 ~ 10). The sorptions on biotite and chlorite show pH dependences, and though high sorptions are found in the pH range less than around 8, gradually decrease in the pH range higher than around 8. No sorptions are found at pH higher than around 8.5. Selenium also shows high sorption on goethite which is one of the weathered products of iron-constituent minerals. Intact and altered granodiorite include biotite, and altered granodiorite and fracture fillings include a small amount of chlorite, but it can be seen that since pH range treated in this study was 9.3 ~ 9.5, Kd values of Se were quite low.

For the sorption of Pu on the rock matrix, Kd values on intact granodiorite are little higher than those on altered granodiorite and fracture fillings. Because the specific surface area of intact granodiorite is smaller than those of other rock matrixes described in 2.4.2, the Kd

values on intact granodiorite per unit surface area are further calculated higher than those of other rock matrixes. The difference in K_d values between three rock matrixes is the rate of constituent biotite. Namely, biotite is contained only in intact granodiorite. It is generally known that K_d of Pu on biotite is high [Releya et al., 1980; Allard, 1982], Pu sorption property is considered to depend on the amount of biotite contained in rock.

4.3 Consideration of a simplified model for D_e

As described in 4.1, D_e values are dependent on both formation factor and D_v . From this fact, a simplified model based on formation factors of the rocks and D_v of species was considered to predict D_e . The authors have proposed the same model on diffusion of Cs^+ , Ni^{2+} and Sm^{3+} in granodiorite, basalt and mudstone, and have approximately explained the measured D_e values even though those rock porosities were smaller than those of the rocks treated in this study [Sato et al., in printing]. Pore sizes larger than 10nm were found in these measurements for granodiorite and mudstone, and pores smaller than 10nm were especially not found. Pore-size distributions obtained in this study also show similar ones to the granodiorite and mudstone reported previously. Therefore, diffusion behaviour of species is predicted to be similar to those rocks. The results of pore-size distributions in the rocks measured in this study indicate that the pore sizes are much larger than diffusing ionic sizes in the porewater and the effect of electrostatic interaction of species with the rock pore surface such as a surface diffusion [Muurinen et al., 1987] and an anion-exclusion [McKinley and Hadermann, 1984] is not significant. Therefore, an empirical equation in porosity dependence of formation factor on all species was derived by the least squares method. Consequently, the empirical equation; $FF = 0.21 \cdot \epsilon - 0.0018$ (correlation coefficient $r = 0.86449$) was obtained.

Effective diffusion coefficients of each species were predicted based on ionic diffusion coefficients in free water and formation factors for each porosity calculated from the empirical equation and compared with the measured values. **Figure 11** shows the predicted and measured D_e values. As shown in **Figure 11**, both D_e values are consistent in a deviation within a factor of about four, and it is concluded that the simplified model based on formation factor and D_v is approximately available to predict D_e .

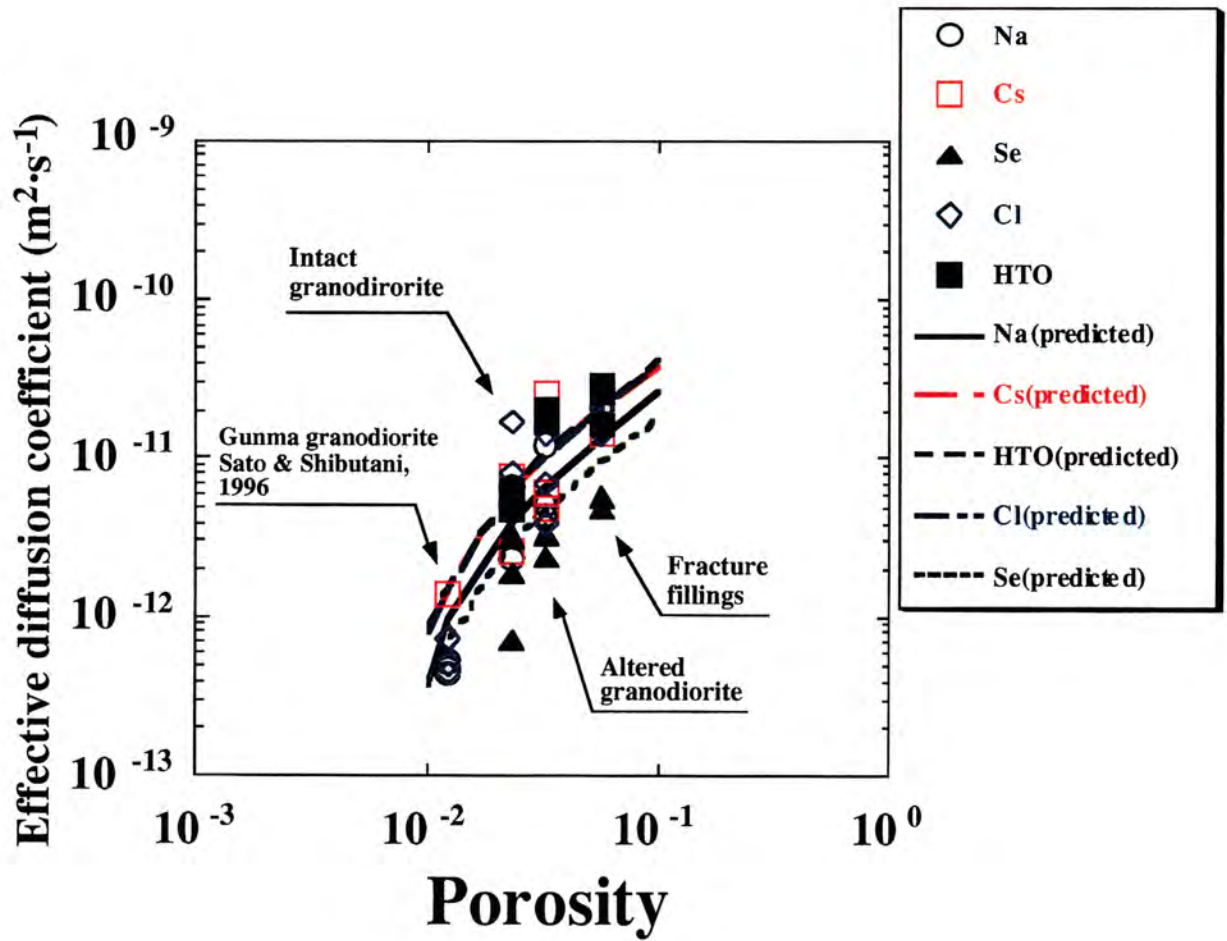


Figure 11 Comparison between D_e values predicted by the model and measured D_e values

5. CONCLUSION

Experimental studies on diffusion of ions into the pore spaces of the rock matrix, sorption of ions on the rock pore surfaces and pore properties were performed, concentrated on fracture type B with a zone of fracture fillings and an altered zone found at the Kamaishi In Situ Test Site to quantify the degree of nuclide retardation in fractured crystalline rock. The results are concluded as follows:

(1) Through-diffusion experiments were carried out to obtain D_e and D_a values for Na, Cs, HTO, Cl and Se as a function of ionic charge through three rocks; fracture fillings, altered and intact granodiorite, composing fracture type B using in situ groundwater as the porewater at 22 ~ 25°C. The effective diffusion coefficients for all elements are in the order of fracture fillings > altered granodiorite > intact granodiorite in proportion to these porosities, and no significant difference between these species in the D_e values was found. The effective diffusion coefficients of these species in the rock matrix could be affected dominantly by those D_v values and porosities for each rock, and are approximately determined by formation factors and D_v values, because the pore sizes are much larger than diffusing ionic sizes and the effect of electrostatic interaction of species with the rock pore surface is not significant. On the other hand, no remarkable dependence on the rock porosity in D_a values is found, and no large variation in the D_a values was found except for HTO which is a non-sorbing nuclide.

(2) Batch sorption experiments for Cs, Sr, Se, ^{238}U and ^{239}Pu were conducted on fracture fillings, altered and intact granodiorite. The experiments only for Se, a redox sensitive element, were carried out in an N_2 -atmospheric glove box ($\text{O}_2 < 1\text{ppm}$) to keep the chemical species. The distribution coefficients of Cs and Sr were in the order of fracture fillings > intact granodiorite \geq altered granodiorite, and Se hardly sorbed on all rock samples. These K_d values were compared with those calculated from through-diffusion experiments. All the K_d values obtained from the diffusion experiments showed a tendency lower than those obtained from batch sorption experiments. The distribution coefficients of Se calculated from diffusion experiments were consistent with those obtained from batch method by converting specific surface areas of the rock samples. However, the converted K_d values for Cs were one order of

magnitude or more higher than those obtained from batch method. A concentration dependence of C_s in K_d on the rock is possible, because tracer concentrations between sorption and diffusion experiments to obtain K_d values had a large difference. Consideration for isotherm of C_s in K_d on the rock is required.

(3) Porosity and density of each rock sample were determined by both a water saturation method and a mercury porosimetry, and pore-size distribution and specific surface area of the pores were measured by the mercury porosimetry. The porosity is in the order of fracture fillings (5.6%) > altered granodiorite (3.2%) > intact granodiorite (2.3%). The pore-size distribution of the intact and altered granodiorite is ranging from 10nm to 0.2mm, and the fracture fillings have that of 50nm to 0.2mm, but a lot of pores were found around 100nm and 0.2mm in the fracture fillings.

(4) Cation exchange capacities for each rock samples were measured. Slight CEC values (about 2 meq/100g) for intact and altered granodiorite were obtained, and those for fracture fillings and mixture of each rock (sample from fracture type C) were measured to be about 17 and 62 meq/100g, respectively. The cause that the CEC values of fracture fillings and the sample from fracture type C were higher than other rock matrixes, is considered to be due to constituent stilbite which has a high CEC.

(5) A simplified model based on formation factors of the rocks and D_v of species was considered to predict D_e . The predicted D_e values were consistent in a deviation within a factor of about four, and it is concluded that the simplified model based on formation factor and D_v is approximately available to predict D_e .

6. ACKNOWLEDGEMENT

The authors would like to thank Messrs. Y. Kohara and N. Uchidate of Inspection Development Company, Ltd. for conducting diffusion experiments and Mis. T. Takahashi of the same company for measuring CEC of rock samples. We would also like to express appreciation to Dr. H. Yoshida of Tono Geoscience Center for constructive comments and discussions.

7. REFERENCES

- [1] Allard, B. (1989):
Sorption of Actinides in Granitic Rock, *KBS TR* 82-12.
- [2] Brookins, D. G. (1988):
Eh-pH Diagrams for Geochemistry, Springer-Verlag Berlin Heidelberg, 18.
- [3] Crank, J. (1975):
The Mathematics of Diffusion, Oxford University Press, Oxford.
- [4] Daniel, D. E., Shackelford, C. D. (1988):
Disposal Barriers That Release Contaminants only by Molecular Diffusion, *Nucl. Chem. Waste Manage.*, 8, 299 ~ 305.
- [5] *Japan Bentonite Manufactures Association Standard* (JBAS, 1977):
JBAS-106-77, 12 ~ 14.
- [6] " *Kagaku-binran* " (*Chemical Handbook*), 2nd ed., The Chemical Society of Japan,
Maruzen, Tokyo (1975) (in Japanese).
- [7] Kita, H., Iwai, T., Nakashima, S. (1989):
Diffusion Coefficient Measurement of an Ion in Pore Water of Granite and Tuff,
Journal of the Japan Society of Engineering Geology, 30-2, 26 ~ 32.
- [8] Kumada, M., Iwai, T., Sagawa, T., Nishiyama, K. (1990):
Diffusion Experiment of a Radionuclide in Granitic Rock Cores, *JAERI-M* 90-179.
- [9] McKinley, I. G., Hadermann, J. (1984):
Radionuclide Sorption Database for Swiss Safety Assessment, *NAGRA Technical Report*, NTB 84-40.
- [10] Monicard, R. P. (1980):
Properties of Reservoir Rocks: Core Analysis, Editions Technip, Paris, France.
- [11] Muurinen, A., Penttilä-Hiltunen, P., Rantanen, J. (1987):
Scientific Basis for Nuclear Waste Management X, 803 ~ 811, Bates, J. K. and Seefeldt, W. B., eds., *Mat. Res. Soc. Symp. Proc.*

- [12] Nishiyama, K., Nakashima, S., Tada, R., Uchida, T. (1990):
Diffusion of an Ion in Rock Porewater and Its Relation to Pore Characteristics,
Mining Geology, 40 (5), 323 ~ 336.
- [13] Osawa, H., Sasamoto, H., Nohara, T., Ota, K., Yoshida, H. (1995):
Development of a Conceptual Flow-Path Model of Nuclide Migration in
Crystalline Rock – A Core Study at the Kamaishi In Situ Test Site, Japan –, Mat.
Res. Soc. Symp. Proc. Vol. 353, 1267 ~ 1273.
- [14] Park, C. K., Han, K. W., Park, H. H. (1991):
High Level Radioactive Waste Management Proceedings Vol. 1, 156 ~ 160.
- [15] Power Reactor and Nuclear Fuel Development Corporation (1993):
PNC Technical Report, PNC TN 1410 93 – 059.
- [16] Releya, J. F. et al. (1980):
Batch Kd Determinations with Common Materials and Representative
Groundwaters, *PNL AS 73 52.*
- [17] Robinson, R. A., Stokes, R. H. (1959):
Electrolyte Solutions, 2nd ed., London Butter Worths, 317.
- [18] Sato, H., Ashida, T., Kohara, Y., Yui, M., Umeki, H., Ishiguro, K. (1992a):
PNC Technical Report, PNC TN 8410 92–164.
- [19] Sato, H., Yui, M., Ishikawa, H. (1992b):
PNC Technical Report, PNC TN 8410 92–222.
- [20] Sato, H., Shibutani, T. (1994):
PNC Technical Report, PNC TN 8410 94–284.
- [21] Sato, H., Shibutani, T. (1996):
PNC Technical Report, PNC TN 1100 96 – 010, 139 ~ 144.
- [22] Sato, H., Shibutani, T., Yui, M. (in printing):
Experimental and Modelling Studies on Diffusion of Cs, Ni and Sm in
Granodiorite, Basalt and Mudstone, *Journal of Contaminant Hydrology.*
- [23] Shachelford, C. D., Daniel, D. E. (1991):
Diffusion in Saturated Soil. I: Background, *J. Geotech. Eng.*, 117 (3), 467 ~
484.

- [24] Shibutani, T., Yui, M., Yoshikawa, H. (1994a):
Sorption Mechanism of Pu, Am and Se on Sodium Bentonite, *Mat. Res. Soc. Symp. Proc.* Vol. 333, 725 ~ 730.
- [25] Shibutani, T., Nishikawa, Y., Inui, S., Uchidate, N., Yui, M. (1994b):
PNC Technical Report, PNC TN 8410 94-395 (in Japanese).
- [26] Skagius, K., Neretnieks, I. (1982):
Scientific Basis for Nuclear Waste Management V, 509 ~ 518, Lutze, W. ed., Plenum Press.
- [27] Suzuki, T., Nakashima, S., Nagano, T., Kita, H. (1989):
Mining Geology, 39 (6), 349 ~ 354 (in Japanese).
- [28] Yamaguchi, T., Sakamoto, Y., Senoo, M. (1992):
Surface Diffusion of Strontium in Rocks, *1992 Annual Meeting of the Atomic Energy Society of Japan, C19* (in Japanese).
- [29] Yamaguchi, T., Isobe, H., Nakayama, S. (1996):
Pore Structure of Inada Granite, *1996 Annual Meeting of the Atomic Energy Society of Japan, M54* (in Japanese).

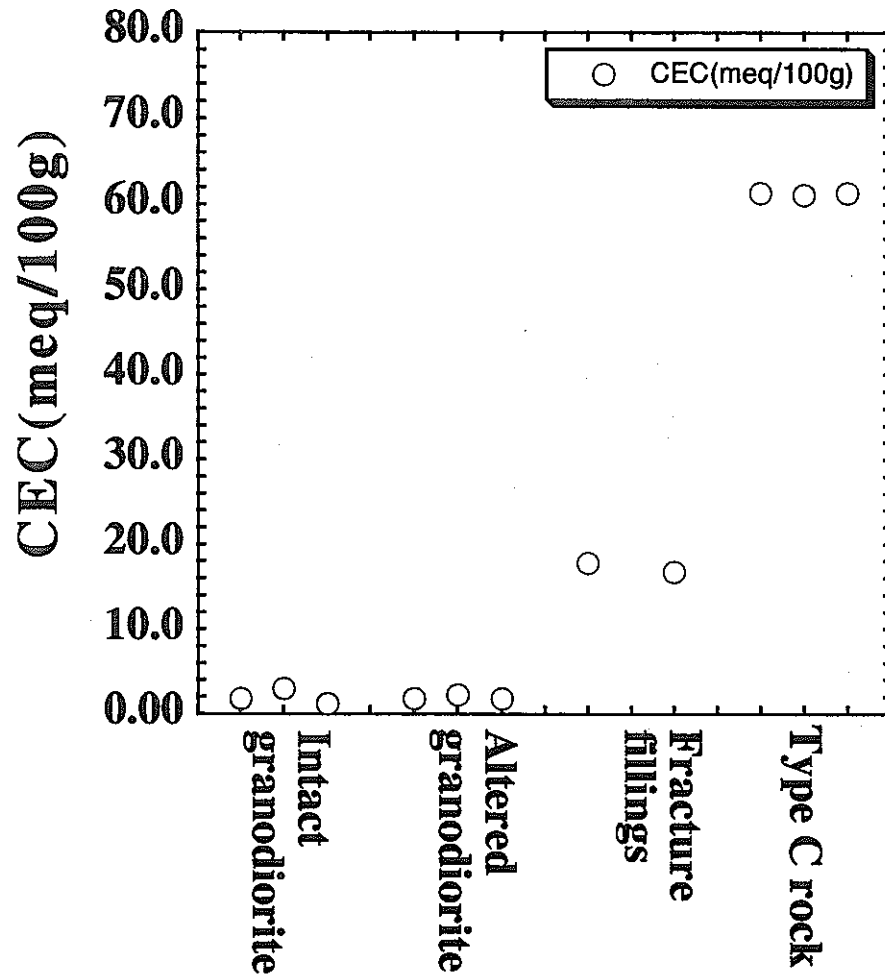
	Rock	Porosity(-)	Ion	Atmosphere	Temperature(°C)	Da(m2/s)	De(m2/s)	α (-)	Kd(ml/g)	G(-)	FF(-)	pH
0	Intact granodiorite	0.023	Na+	aerobic	25.0	8.0e-11	6.5e-12	0.0850	0.023	0.212	4.88e-03	8.70
1	Intact granodiorite	0.023	Na+	aerobic	25.0		2.3e-12			0.0752	1.73e-03	8.70
2	Intact granodiorite	0.023	Na+	aerobic	25.0	5.4e-12	5.2e-12	0.960	0.34	0.170	3.91e-03	8.70
3	Intact granodiorite	0.023	Cs+	aerobic	25.0	1.2e-11	7.8e-12	0.650	0.23	0.165	3.80e-03	8.70
4	Intact granodiorite	0.023	Cs+	aerobic	25.0	1.3e-11	2.5e-12	0.190	0.062	0.0530	1.22e-03	8.70
5	Intact granodiorite	0.023	Cs+	aerobic	25.0	7.1e-12	5.0e-12	0.700	0.25	0.106	2.44e-03	8.70
6	Intact granodiorite	0.023	HTO	aerobic	23.0	2.2e-10	5.0e-12	0.00	0.0	0.102	2.35e-03	8.70
7	Intact granodiorite	0.023	HTO	aerobic	23.0	2.1e-10	4.8e-12	0.00	0.0	0.0975	2.24e-03	8.70
8	Intact granodiorite	0.023	HTO	aerobic	23.0	1.9e-10	6.2e-12	0.0330	0.0037	0.126	2.90e-03	8.70
9	Intact granodiorite	0.023	Cl-	aerobic	25.0	5.6e-12	1.7e-11	3.00	1.1	0.360	8.28e-03	8.70
10	Intact granodiorite	0.023	Cl-	aerobic	25.0	6.7e-12	8.1e-12	1.20	0.43	0.173	3.98e-03	8.70
11	Intact granodiorite	0.023	Cl-	aerobic	25.0	1.7e-11	4.8e-12	0.280	0.094	0.103	2.37e-03	8.70
12	Intact granodiorite	0.023	SeO32-	anaerobic	22.1	1.0e-11	3.2e-12	0.320	0.11	0.145	3.34e-03	9.29
13	Intact granodiorite	0.023	SeO32-	anaerobic	22.1	4.3e-12	7.2e-13	0.170	0.054	0.0330	7.50e-04	9.29
14	Intact granodiorite	0.023	SeO32-	anaerobic	22.1	5.3e-12	1.9e-12	0.360	0.12	0.0861	1.98e-03	9.29
15												
16	Altered granodiorite	0.032	Na+	aerobic	25.0	8.4e-12	1.2e-11	1.43	0.54	0.282	9.02e-03	8.77
17	Altered granodiorite	0.032	Na+	aerobic	25.0	7.7e-12	5.1e-12	0.660	0.24	0.167	5.34e-03	8.77
18	Altered granodiorite	0.032	Na+	aerobic	25.0	1.3e-11	4.3e-12	0.330	0.11	0.101	3.23e-03	8.77
19	Altered granodiorite	0.032	Cs+	aerobic	25.0	3.2e-12	2.5e-11	0.700	0.25	0.381	1.22e-02	8.77
20	Altered granodiorite	0.032	Cs+	aerobic	25.0	5.3e-12	4.8e-12	0.910	0.34	0.0732	2.34e-03	8.77
21	Altered granodiorite	0.032	Cs+	aerobic	25.0	5.1e-12	6.0e-12	1.20	0.45	0.0915	2.93e-03	8.77
22	Altered granodiorite	0.032	HTO	aerobic	23.0	5.3e-10	1.7e-11	0.00	0.0	0.248	7.94e-03	8.77
23	Altered granodiorite	0.032	HTO	aerobic	23.0	6.3e-10	2.0e-11	0.00	0.0	0.292	9.34e-03	8.77
24	Altered granodiorite	0.032	HTO	aerobic	23.0	5.3e-10	1.7e-11	0.00	0.0	0.248	7.94e-03	8.77
25	Altered granodiorite	0.032	Cl-	aerobic	25.0	5.7e-12	1.4e-11	2.50	0.95	0.216	6.91e-03	8.77
26	Altered granodiorite	0.032	Cl-	aerobic	25.0	5.5e-12	6.9e-12	1.30	0.49	0.106	3.39e-03	8.77
27	Altered granodiorite	0.032	Cl-	aerobic	25.0	2.0e-11	3.9e-12	0.200	0.064	0.0600	1.92e-03	8.77
28	Altered granodiorite	0.032	SeO32- *	anaerobic	21.9	1.4e-12						9.33
29	Altered granodiorite	0.032	SeO32-	anaerobic	21.9	1.3e-11	2.4e-12	0.180	0.057	0.0781	2.50e-03	9.33
30	Altered granodiorite	0.032	SeO32-	anaerobic	21.9	9.3e-12	3.3e-12	0.350	0.12	0.107	3.42e-03	9.33
31												
32	Fracture fillings	0.056	Na+	aerobic	25.0	1.9e-11	2.1e-11	1.11	0.43	0.282	1.58e-02	8.92
33	Fracture fillings	0.056	Na+	aerobic	25.0	2.0e-11	1.7e-11	0.850	0.33	0.228	1.28e-02	8.92
34	Fracture fillings	0.056	Na+	aerobic	25.0							
35	Fracture fillings	0.056	Cs+	aerobic	25.0	1.1e-11	1.4e-11	1.30	0.51	0.122	6.83e-03	8.92
36	Fracture fillings	0.056	Cs+	aerobic	25.0	1.3e-11	2.2e-11	1.70	0.68	0.192	1.08e-02	8.92
37	Fracture fillings	0.056	Cs+	aerobic	25.0							
38	Fracture fillings	0.056	HTO	aerobic	23.0	4.8e-10	2.7e-11	0.0560	0.0	0.225	1.26e-02	8.92
39	Fracture fillings	0.056	HTO	aerobic	23.0	5.0e-10	2.8e-11	0.0560	0.0	0.244	1.37e-02	8.92
40	Fracture fillings	0.056	HTO	aerobic	23.0	2.9e-10	1.6e-11	0.0550	0.0	0.139	7.78e-03	8.92

	Rock	Porosity(-)	Ion	Atmosphere	Temperature(°C)	Da(m ² /s)	De(m ² /s)	α(-)	Kd(ml/g)	G(-)	FF(-)	pH
41	Fracture fillings	0.056	Cl-	aerobic	25.0	1.8e-11	2.1e-11	1.20	0.47	0.185	1.04e-02	8.92
42	Fracture fillings	0.056	Cl-	aerobic	25.0	3.4e-11	1.4e-11	0.410	0.15	0.123	6.89e-03	8.92
43	Fracture fillings	0.056	Cl-	aerobic	25.0							
44	Fracture fillings	0.056	SeO32-	anaerobic		8.1e-12	5.7e-12	0.700	0.27	0.106	5.94e-03	9.56
45	Fracture fillings	0.056	SeO32-	anaerobic		3.7e-12	4.9e-12	1.31	0.52	0.0911	5.10e-03	9.50
46	Fracture fillings	0.056	SeO32-	anaerobic								
47												
48	*D.L.: 1.4e-12m ² /s											

PNC TN8410 97-127

	Rock	Sample No.	Na+(meq/100g)	K+(meq/100g)	Ca2+(meq/100g)	Mg2+(meq/100g)	Al(mol/100g) 1)	Si(mol/100g)	Cl-(meq/100g) 2)	SO42-(meq/100g) 3)	CEC(meq/100g)
0	Intact granodiorite	FG-1	26.000	15.30	498.900	16.40	0.000	7.100	11.20	0.000	1.800
1	Intact granodiorite	FG-2	26.000	15.30	459.000	16.40	0.000	3.600	16.90	0.000	3.000
2	Intact granodiorite	FG-3	26.000	15.30	468.900	16.40	0.000	5.300	16.90	0.000	1.200
3											
4	Altered granodiorite	AG-1	69.500	25.50	3231.10	32.80	0.000	5.300	56.30	16.60	1.800
5	Altered granodiorite	AG-2	104.30	25.50	3193.40	32.90	0.000	7.100	129.7	16.60	2.200
6	Altered granodiorite	AG-3	78.200	25.50	3113.20	32.90	0.000	7.100	62.00	16.60	1.800
7											
8	Fracture fillings	FMB-1	217.30	25.50	23639.6	32.80	0.000	42.70	0.000	0.000	17.80
9	Fracture fillings	FMB-2	217.40	25.50	24443.4	32.90	0.000	42.70	0.000	0.000	
10	Fracture fillings	FMB-3	217.30	25.50	23541.2	32.80	0.000	49.80	0.000	0.000	16.80
11											
12	Type C rock	FMC-1	1051.6	61.30	6561.00	65.70	0.000	35.55	78.90	29.10	61.30
13	Type C rock	FMC-2	1000.0	61.30	6604.70	65.80	0.000	35.58	0.000	24.90	61.10
14	Type C rock	FMC-3	1017.3	61.30	6674.00	65.80	0.000	35.58	0.000	16.60	61.30
15											
16											
17	1)D.L.:0.15mmol/100g										
18	2)D.L.:0.11mmol/100g										
19	3)D.L.:0.17mmol/100g										

PNC TN8410 97-127



Appendix 3 Relation between CEC values and rock facies

	Species	Solid	Initial conc.(M)	Initial conc.(ppm)	Liquid/solid ratio(ml/g)	Atmosphere	Temperature(°C)	pH	Contact time(day)	Kd(ml/g)
0	Cs+	Intact granodiorite	8.58e-05	1.14e+01	100.00	aerobic	23.0	9.380	30.0	28.00
1	Cs+	Intact granodiorite	8.58e-05	1.14e+01	100.00	aerobic	23.0	9.380	30.0	29.00
2	Cs+	Intact granodiorite	8.58e-05	1.14e+01	100.00	aerobic	23.0	9.380	30.0	29.00
3	Cs+	Altered granodiorite	8.58e-05	1.14e+01	100.00	aerobic	23.0	9.480	30.0	17.00
4	Cs+	Altered granodiorite	8.58e-05	1.14e+01	100.00	aerobic	23.0	9.480	30.0	18.00
5	Cs+	Altered granodiorite	8.58e-05	1.14e+01	100.00	aerobic	23.0	9.480	30.0	18.00
6	Cs+	Fracture fillings	8.58e-05	1.14e+01	100.00	aerobic	23.0	9.440	30.0	96.00
7	Cs+	Fracture fillings	8.58e-05	1.14e+01	100.00	aerobic	23.0	9.440	30.0	107.0
8	Cs+	Fracture fillings	8.58e-05	1.14e+01	100.00	aerobic	23.0	9.400	30.0	111.0
9										
10	Sr2+	Intact granodiorite	9.13e-05	8.00e+00	100.00	aerobic	23.0	9.430	30.0	27.00
11	Sr2+	Intact granodiorite	9.13e-05	8.00e+00	100.00	aerobic	23.0	9.430	30.0	38.00
12	Sr2+	Intact granodiorite	9.13e-05	8.00e+00	100.00	aerobic	23.0	9.430	30.0	44.00
13	Sr2+	Altered granodiorite	9.13e-05	8.00e+00	100.00	aerobic	23.0	9.450	30.0	36.00
14	Sr2+	Altered granodiorite	9.13e-05	8.00e+00	100.00	aerobic	23.0	9.450	30.0	36.00
15	Sr2+	Altered granodiorite	9.13e-05	8.00e+00	100.00	aerobic	23.0	9.450	30.0	36.00
16	Sr2+	Fracture fillings	9.13e-05	8.00e+00	100.00	aerobic	23.0	9.420	30.0	48.00
17	Sr2+	Fracture fillings	9.13e-05	8.00e+00	100.00	aerobic	23.0	9.420	30.0	50.00
18	Sr2+	Fracture fillings	9.13e-05	8.00e+00	100.00	aerobic	23.0	9.420	30.0	53.00
19										
20	SeO32-	Intact granodiorite	1.00e-04	7.90e+00	20.000	anaerobic		9.270	30.0	0.000
21	SeO32-	Intact granodiorite	1.00e-04	7.90e+00	20.000	anaerobic		9.320	30.0	0.9400
22	SeO32-	Intact granodiorite	1.00e-04	7.90e+00	20.000	anaerobic		9.310	30.0	0.6200
23	SeO32-	Altered granodiorite	1.00e-04	7.90e+00	20.000	anaerobic		9.360	30.0	0.3000
24	SeO32-	Altered granodiorite	1.00e-04	7.90e+00	20.000	anaerobic		9.370	30.0	0.9400
25	SeO32-	Altered granodiorite	1.00e-04	7.90e+00	20.000	anaerobic		9.400	30.0	1.610
26	SeO32-	Fracture fillings	1.00e-04	7.90e+00	20.000	anaerobic		9.280	30.0	0.6200
27	SeO32-	Fracture fillings	1.00e-04	7.90e+00	20.000	anaerobic		9.280	30.0	1.270
28	SeO32-	Fracture fillings	1.00e-04	7.90e+00	20.000	anaerobic		9.300	30.0	1.610
29										
30	UO2(CO3)34-	Intact granodiorite	1.07e-06	2.55e-01	100.00	aerobic	23.0	9.110	30.0	2.000
31	UO2(CO3)34-	Intact granodiorite	1.07e-06	2.55e-01	100.00	aerobic	23.0	9.110	30.0	3.000
32	UO2(CO3)34-	Intact granodiorite	1.07e-06	2.55e-01	100.00	aerobic	23.0	9.110	30.0	9.000
33	UO2(CO3)34-	Altered granodiorite	1.07e-06	2.55e-01	100.00	aerobic	23.0	9.110	30.0	2.000
34	UO2(CO3)34-	Altered granodiorite	1.07e-06	2.55e-01	100.00	aerobic	23.0	9.110	30.0	3.000
35	UO2(CO3)34-	Altered granodiorite	1.07e-06	2.55e-01	100.00	aerobic	23.0	9.110	30.0	7.000
36	UO2(CO3)34-	Fracture fillings	1.07e-06	2.55e-01	100.00	aerobic	23.0	9.110	30.0	3.000
37	UO2(CO3)34-	Fracture fillings	1.07e-06	2.55e-01	100.00	aerobic	23.0	9.110	30.0	7.000
38	UO2(CO3)34-	Fracture fillings	1.07e-06	2.55e-01	100.00	aerobic	23.0	9.110	30.0	9.000
39										
40	UO2(CO3)34-	Intact granodiorite	1.09e-06	2.59e-01	100.00	aerobic	23.0		30.0	2.000

PNC TN8410 97-127

	Species	Solid	Initial conc.(M)	Initial conc.(ppm)	Liquid/solid ratio(ml/g)	Atmosphere	Temperature(°C)	pH	Contact time(day)	Kd(ml/g)
41	UO2(CO3)34-	Intact granodiorite	1.09e-06	2.59e-01	100.00	aerobic	23.0		30.0	2.000
42	UO2(CO3)34-	Intact granodiorite	1.09e-06	2.59e-01	100.00	aerobic	23.0		30.0	4.000
43	UO2(CO3)34-	Altered granodiorite	1.09e-06	2.59e-01	100.00	aerobic	23.0		30.0	1.000
44	UO2(CO3)34-	Altered granodiorite	1.09e-06	2.59e-01	100.00	aerobic	23.0		30.0	7.000
45	UO2(CO3)34-	Altered granodiorite	1.09e-06	2.59e-01	100.00	aerobic	23.0		30.0	13.00
46	UO2(CO3)34-	Fracture fillings	1.09e-06	2.59e-01	100.00	aerobic	23.0		30.0	4.000
47	UO2(CO3)34-	Fracture fillings	1.09e-06	2.59e-01	100.00	aerobic	23.0		30.0	13.00
48	UO2(CO3)34-	Fracture fillings	1.09e-06	2.59e-01	100.00	aerobic	23.0		30.0	18.00
49										
50	UO2(CO3)34-	Intact granodiorite	6.27e-07	1.49e-01	100.00	aerobic	23.0		30.0	0.000
51	UO2(CO3)34-	Intact granodiorite	6.27e-07	1.49e-01	100.00	aerobic	23.0		30.0	4.000
52	UO2(CO3)34-	Intact granodiorite	6.27e-07	1.49e-01	100.00	aerobic	23.0		30.0	6.000
53	UO2(CO3)34-	Altered granodiorite	6.27e-07	1.49e-01	100.00	aerobic	23.0		30.0	0.000
54	UO2(CO3)34-	Altered granodiorite	6.27e-07	1.49e-01	100.00	aerobic	23.0		30.0	4.000
55	UO2(CO3)34-	Altered granodiorite	6.27e-07	1.49e-01	100.00	aerobic	23.0		30.0	4.000
56	UO2(CO3)34-	Fracture fillings	6.27e-07	1.49e-01	100.00	aerobic	23.0		30.0	3.000
57	UO2(CO3)34-	Fracture fillings	6.27e-07	1.49e-01	100.00	aerobic	23.0		30.0	8.000
58	UO2(CO3)34-	Fracture fillings	6.27e-07	1.49e-01	100.00	aerobic	23.0		30.0	9.000
59										
60	UO2(CO3)34-	Intact granodiorite	1.00e-06	2.38e-01	100.00	aerobic	23.0	8.420	30.0	0.000
61	UO2(CO3)34-	Intact granodiorite	1.00e-06	2.38e-01	100.00	aerobic	23.0	8.420	30.0	4.000
62	UO2(CO3)34-	Intact granodiorite	1.00e-06	2.38e-01	100.00	aerobic	23.0	8.420	30.0	9.000
63	UO2(CO3)34-	Altered granodiorite	1.00e-06	2.38e-01	100.00	aerobic	23.0	8.650	30.0	0.000
64	UO2(CO3)34-	Altered granodiorite	1.00e-06	2.38e-01	100.00	aerobic	23.0	8.650	30.0	0.000
65	UO2(CO3)34-	Altered granodiorite	1.00e-06	2.38e-01	100.00	aerobic	23.0	8.650	30.0	0.000
66	UO2(CO3)34-	Fracture fillings	1.00e-06	2.38e-01	100.00	aerobic	23.0	8.880	30.0	3.000
67	UO2(CO3)34-	Fracture fillings	1.00e-06	2.38e-01	100.00	aerobic	23.0	8.880	30.0	3.000
68	UO2(CO3)34-	Fracture fillings	1.00e-06	2.38e-01	100.00	aerobic	23.0	8.880	30.0	6.000
69										
70	UO2(CO3)34-	Intact granodiorite	1.05e-06	2.50e-01	1000.0	aerobic	23.0	9.450	30.0	12.00
71	UO2(CO3)34-	Intact granodiorite	1.05e-06	2.50e-01	1000.0	aerobic	23.0	9.450	30.0	25.00
72	UO2(CO3)34-	Intact granodiorite	1.05e-06	2.50e-01	1000.0	aerobic	23.0	9.450	30.0	25.00
73	UO2(CO3)34-	Altered granodiorite	1.05e-06	2.50e-01	1000.0	aerobic	23.0	9.460	30.0	51.00
74	UO2(CO3)34-	Altered granodiorite	1.05e-06	2.50e-01	1000.0	aerobic	23.0	9.460	30.0	51.00
75	UO2(CO3)34-	Altered granodiorite	1.05e-06	2.50e-01	1000.0	aerobic	23.0	9.460	30.0	69.00
76	UO2(CO3)34-	Fracture fillings	1.05e-06	2.50e-01	1000.0	aerobic	23.0	9.480	30.0	38.00
77	UO2(CO3)34-	Fracture fillings	1.05e-06	2.50e-01	1000.0	aerobic	23.0	9.480	30.0	83.00
78	UO2(CO3)34-	Fracture fillings	1.05e-06	2.50e-01	1000.0	aerobic	23.0	9.480	30.0	142.0
79										
80	Pu(CO3)32-	Intact granodiorite	1.55e-09	3.70e-04	100.00	aerobic	24.0	8.600	66.0	3230
81	Pu(CO3)32-	Intact granodiorite	1.55e-09	3.70e-04	100.00	aerobic	24.0	8.600	66.0	5210

	Species	Solid	Initial conc.(M)	Initial conc.(ppm)	Liquid/solid ratio(ml/g)	Atmosphere	Temperature(°C)	pH	Contact time(day)	Kd(ml/g)
82	Pu(CO3)32-	Altered granodiorite	1.55e-09	3.70e-04	100.00	aerobic	24.0	8.600	66.0	3230
83	Pu(CO3)32-	Altered granodiorite	1.55e-09	3.70e-04	100.00	aerobic	24.0	8.600	66.0	2560
84	Pu(CO3)32-	Fracture fillings	1.55e-09	3.70e-04	100.00	aerobic	24.0	8.600	66.0	1770
85	Pu(CO3)32-	Fracture fillings	1.55e-09	3.70e-04	100.00	aerobic	24.0	8.600	66.0	1360

	Rock	Method	Depth(m)	Porosity(%)	Natural dry density(kg/m3)	Saturation density(kg/m3)	Dry density(kg/m3)	Specific surce area(m2/g)
0	Intact granodiorite	Mercury	700.00	3.00			2700.0	0.600
1	Intact granodiorite	Mercury	700.00	2.40			2700.0	0.200
2	Intact granodiorite	Mercury	700.00	3.00			2800.0	0.500
3	Intact granodiorite	Water	700.00	2.80			2610.0	
4	Intact granodiorite	Water	700.00	1.20			2770.0	
5	Intact granodiorite	Water	70.000	1.70			2700.0	
6	Intact granodiorite	Water	700.00	1.10			2850.0	
7								
8	Altered granodiorite	Mercury	700.00	2.30			2600.0	0.600
9	Altered granodiorite	Mercury	700.00	3.40			2600.0	0.600
10	Altered granodiorite	Mercury	700.00	3.90			2600.0	0.600
11	Altered granodiorite	Water	700.00	3.30			2620.0	
12	Altered granodiorite	Water	700.00	3.30			2580.0	
13	Altered granodiorite	Water	70.000	3.20			2650.0	
14	Altered granodiorite	Water	700.00	3.40			2610.0	
15								
16	Fracture fillings	Mercury	700.00	3.80			2500.0	0.400
17	Fracture fillings	Mercury	700.00	4.30			2400.0	0.700
18	Fracture fillings	Mercury	700.00	5.30			2400.0	0.400
19	Fracture fillings	Water	700.00	7.40			2350.0	
20	Fracture fillings	Water	700.00	3.70			2840.0	
21	Fracture fillings	Water	70.000	5.80			2180.0	
22	Fracture fillings	Water	700.00	9.60			2260.0	

PNC TN8410 97-127